minutes. The cells were loaded on lymphocyte separation medium (Ficoll-Conray, Immuno-Biologic Laboratories, Gunma, Japan), and centrifuged at 2,000 rpm for 20 minutes. PBMC were collected from the intermediate layer of Ficoll-Conray density gradient centrifugation and washed twice with PBS. The plasma was subjected to heat-inactivation and stored at -20°C until use. A cell separator (COBE-Spectra, GANBRO, Stockholm, Sweden) was used for leukapheresis. Any residual mononuclear cells were collected from apheresis tubes and bags by washing with PBS after cells were collected for clinical transplantation, and separated by Ficoll-Conray density gradient centrifugation. The apheresis plasma was also collected from the collection bags.

Expansion of Vα24$^+$ NKT Cells

In this manuscript, we use the term Vα24$^+$ NKT cells to refer to Vα24$^+$ CD3$^+$ double-positive NKT cells and confirmed the co-expression of Vβ11 chain. Isolated PBMC were cultured in 6-well culture plates (Costar, Corning, NY) at 2.0×10^5 cells/mL (each well filled with 4 mL media) in AIM-V media (Life Technologies, Rockville, MD) containing 10% autologous plasma, supplemented with 100 ng/mL α-galactosylceramide (α-GalCer, supplied by Kirin Brewery Co., Tokyo, Japan) and 100 IU/mL recombinant human (rh) IL-2 (R&D Systems, Minneapolis, MN) for 12 days. IL-2 was freshly added every 3 days to maintain its biologic activity. In the first experiment to define the efficacy for Vα24$^+$ NKT cells expansion between before and after G-CSF mobilization, we used steady-state autologous plasma before G-CSF administration (pre-G-CSF), autologous plasma derived from PB after G-CSF administration (post-G-CSF PB) and autologous plasma obtained from apheresis product after G-CSF administration (post-G-CSF apheresis). In other experiments, we uniformly used autologous plasma obtained from apheresis product.

Monoclonal Antibodies

For flow cytometry analysis, anti-CD3-APC, anti-CD14-FITC, anti-CD16-PE, anti-CD56-FITC, anti-CD161-PE, anti-CD20-FITC and anti-CD19-PE monoclonal antibodies (mAbs) were purchased from BD Biosciences (Mountain View, CA). IgG1-FITC and IgG1-PE (cocktail), anti-Vα 24-FITC, anti-Vα24-PE, anti-Vβ11-PE and anti-CD4$^-$FITC and anti-CD8$^-$PE (cocktail) mAbs were from Immunotech (Marseilles, France). Anti-CD3-FITC mAb was from BD Pharmingen (San Diego, CA). For cell separation, anti-CD34-FITC, anti-CD56-FITC and anti-CD14-FITC mAbs were purchased from BD Biosciences (Mountain View, CA). Anti-Vα24-FITC mAb was from Immunotech (Marseilles, France). Anti-CD3-FITC mAb was from BD Pharmingen (San Diego, CA).

Cell Surface Antigen Analysis

For cell surface antigen staining, cells were incubated with FITC-, PE- or APC- conjugated mouse anti-human mAbs for 30 minutes on ice. After staining, cells were washed twice and re-suspended in PBS. Staining with propidium iodide (PI; Sigma-Aldrich, St. Louis, MO) preceded all experiments to remove dead cells. Data were acquired by flow cytometry (FACSCalibur; BD Biosciences) and analyzed using CellQuest software (BD Biosciences). In this manuscript, we considered "CD56$^+$ cells" as NK cells and use the phrase "CD56$^+$ NK" cells.

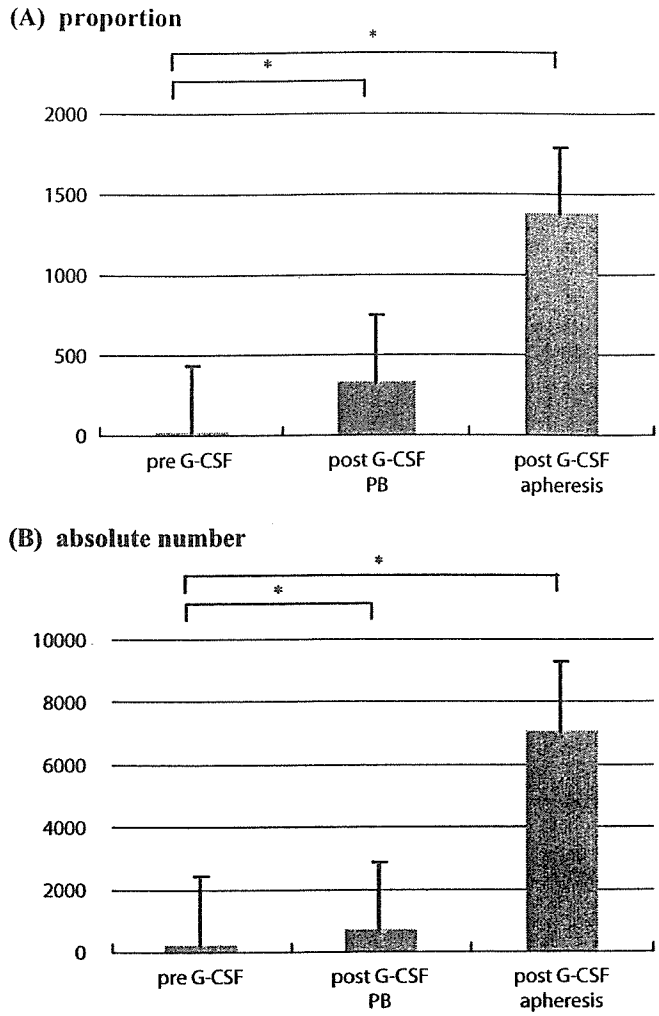

FIGURE 1. Proportion and absolute number of Vα24$^+$ NKT cells on day 12 The proportion (A) and absolute number (B) of Vα24$^+$ NKT cells increased 18(SD±23)- and 182(±158)-fold at the end of 12 days of culture for cells harvested before G-CSF administration, whereas these values were 333(±347)- and 669(±925)-fold in cells harvested after treatment with G-CSF. The highest increase was observed with apheresis product, which showed values of 1384(±1434)- to 7091(±2160)-fold respectively. The results were based on data obtained from 20 healthy donors. The bar means standard deviation. (*; $P<0.05$)

Cell Separation and Coculture

PBSC Obtained from apheresis products were stained with FITC-conjugated mAbs against CD34,

Vα24, CD14, and CD56 for 20 minutes at 4°C and washed once with 5 mM EDTA-PBS. Anti-FITC-microbeads (Miltenyl Biotec, Gladbach, Germany) were then added to PBSC. After target cells were reacted with anti-FITC-microbeads, they were sorted by a magnetic cell separation system (Super MACS; Miltenyl Biotec), according to the manufacturer's protocol. The purity of isolated cells in the positive fraction was monitored and assured to be higher than 90% by flow cytometry, except for $V\alpha24^+$ NKT cells, which are difficult to obtain in high purity because of their rarity in PB. Although $V\alpha24^+$ NKT cells had a low purity (20% at most) after isolation by MACS, they were still considered enriched $V\alpha24^+$ NKT cells. On the other hand, contamination by $CD14^+$, $CD\ 56^+$, $CD34^+$, or $V\alpha24^+$ cells in their respective negative fractions was less than 10%.

To evaluate the influence of each cell population on $V\alpha24^+$ NKT cell expansion, we depleted and/or added back $CD34^+$ cells, $V\alpha24^+$ NKT cells, $CD14^+$ cells or $CD56^+$ NK cells, and evaluated the results on days 3, 6, 9 and 12. To evaluate the direct cell-cell interaction between $CD56^+$ NK cells and others, we used a Cell Culture Insert System with a 3 μm-pore membrane (Transwell, Corning, NY), and placed the $CD56^+$ NK fraction in the upper chamber and the $CD56^-$ fraction in the lower chamber. On day 12, the cells in the lower chamber were analyzed.

Contribution of $CD14^+$ Cells to $V\alpha24^+$ NKT Cell Expansion

To evaluate the contribution of $CD14^+$ cells to $V\alpha24^+$ NKT cell expansion and to optimize the $CD14^+$ cell conditions in our culture system, we depleted and added back $CD14^+$ cells to $CD14^-$ cells on day 0, on day 3, on day 6 or on day 9. $CD14^+$ cell was depleted by MACS (described above) and each added-back cells were 4.0×10^5 cells with optimized medium to maintain final concentration of IL-2 and autologous plasma. We also evaluated changes of concentration of $CD14^+$ cells before and after G-CSF administration and also evaluated the effects of them between different $CD14^+$ cell/$CD14^-$ cell ratio on $V\alpha24^+$ NKT cell expansion using the following culture conditions. The whole cell number was adjusted to 2.0×10^5 cells/ml in all wells, and the ratio of $CD14^+$

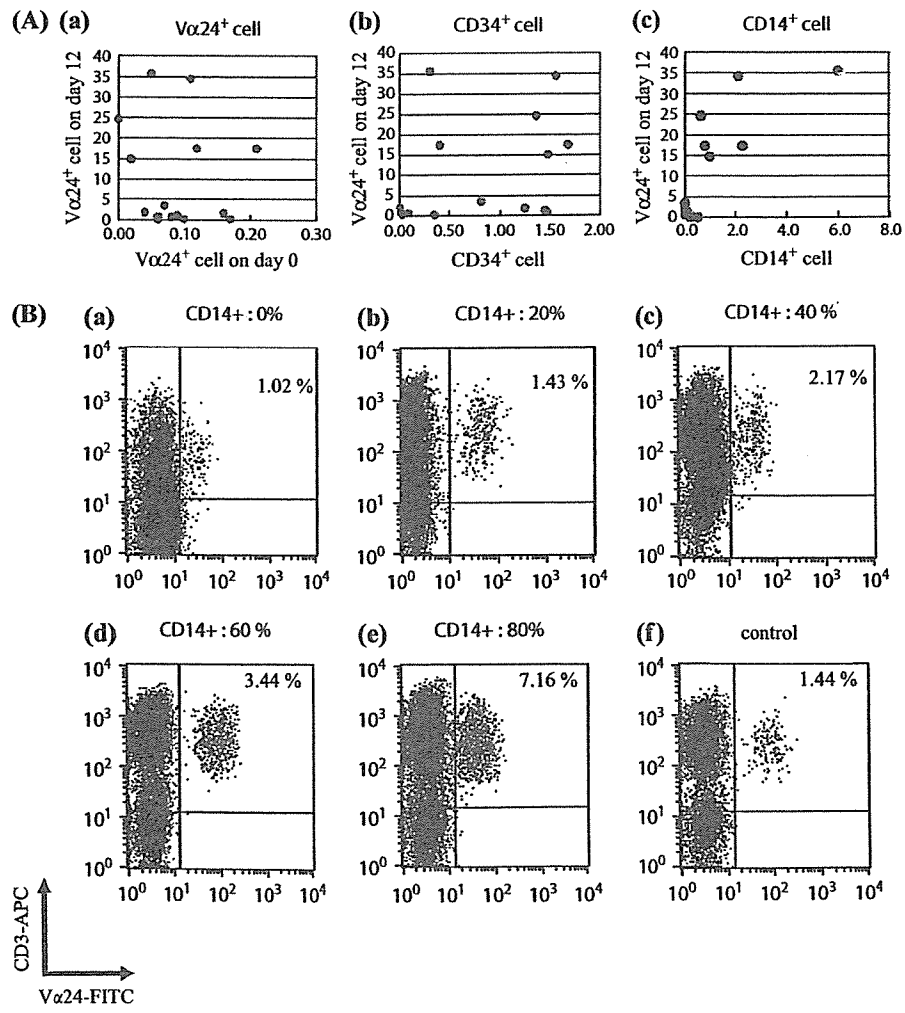

FIGURE 2. Effect of $CD34^+$, $V\alpha24^+$, and $CD14^+$ cells on expansion of $V\alpha24^+$ NKT cells (A) The proportion of (a) $CD34^+$, (b) $V\alpha24^+$ on day 0 were not associated with the expansion efficacy of $V\alpha24^+$ NKT cells ($r^2 = 0.171$, 0.016, respectively). Only $CD14^+$ cells (c) in the initial cell mixture had a relatively strong correlation ($r^2 = 0.545$) with the proliferation of cultured $V\alpha24^+$ NKT cells. These results were analyzed in 16 healthy donors. (B) The efficacy of $V\alpha24^+$ NKT expansion depended on the proportion of $CD14^+$ cells in apheresis products. The proportion of $CD14^+$ cells was as follows: (a) 0, (b) 20, (c) 40, (d) 60 and (e) 80% with a fixed total cell number of 2.0×10^5 cells/ml. The control means the result by using apheresis product without manupiration. These results are representative data from four experiments.

cells: $CD14^-$ cells was 0:5, 1:4, 2:3, 3:2, 4:1 or 5:0. The purpose of these manipulation was to detect the contribution of $CD14^+$ cells in the different timing of culture process and by the different proportion.

Modification of IL-2 Supplementation Schedule

In our original protocol established by Mikami and Harada, we added IL-2 to the cell culture medium every 3 days to maintain its biologic activity. However, in this study, we modified the schedule of IL-2 administration to determine the suitable culture conditions for $V\alpha24^+$ NKT expansion as follows: addition of IL-2 i) only on day 0, ii) days 0 and 3, iii) days 0, 3 & 6, and iv) days 0, 3, 6 & 9. Each supplementation of IL-2 was oriented to 100 IU/mL as a final concentration. The cell numbers and their phenotypes were analyzed on day 12. α-GalCer was also supplemented at final concentration 100 ng/mL.

Statistical Analysis

Student's t test was used to compare 2 groups and P values of < 0.05 were considered statistically significant. Correlation was estimated by the ordinary least squares method. Correlation coefficients are shown as squared values (r^2).

RESULTS

Efficient Expansion of $V\alpha24^+$ NKT Cells Derived from G-CSF-Mobilized PBSCT of Normal Healthy Donors

We compared the expansion-fold of $V\alpha24^+$ NKT cells in PBSCT before and after G-CSF mobilization in 20 healthy donors. The expansion fold of percentage and absolute number of $V\alpha24^+$ NKT cells increased, respectively, 18(SD ± 23)- and 182(± 158)-fold in PBMC before G-CSF mobilization, whereas these were 333(± 347)- and 669(± 925)-fold in G-CSF-mobilized PBMC. Apheresis products from collection bags showed more efficient expansion capacities, from 1384(± 1434)- to 7091(± 2160)-fold (Figs. 1A, B). Thus, G-CSF mobilization significantly increased the capacity for $V\alpha24^+$ NKT cell expansion.

Relationship Between the Concentration of $CD34^+$, $V\alpha24^+$ and $CD14^+$ Cells on V α 24^+ NKT Expansion

To analyze the contribution of $CD34^+$, $V\alpha24^+$ and $CD14^+$ cells on the proliferation of $V\alpha24^+$ NKT cells in apheresis product, we compared the percentage of $CD34^+$, $V\alpha24^+$ and $CD14^+$ cells on day 0 and $V\alpha24^+$ NKT expansion efficacy on day 12. The results suggested only $CD14^+$ cells showed the correlation with the expansion of $V\alpha24^+$ NKT cells. (Fig. 2A).

Contribution of $CD14^+$ Cells to the Ex Vivo Expansion of $V\alpha24^+$ NKT Cells

It has been reported that $CD14^+$ cells, dendritic cells and monocytes play a critical role in the initiation of proliferation of $V\alpha24^+$ NKT cells.[9] In PB after G-CSF

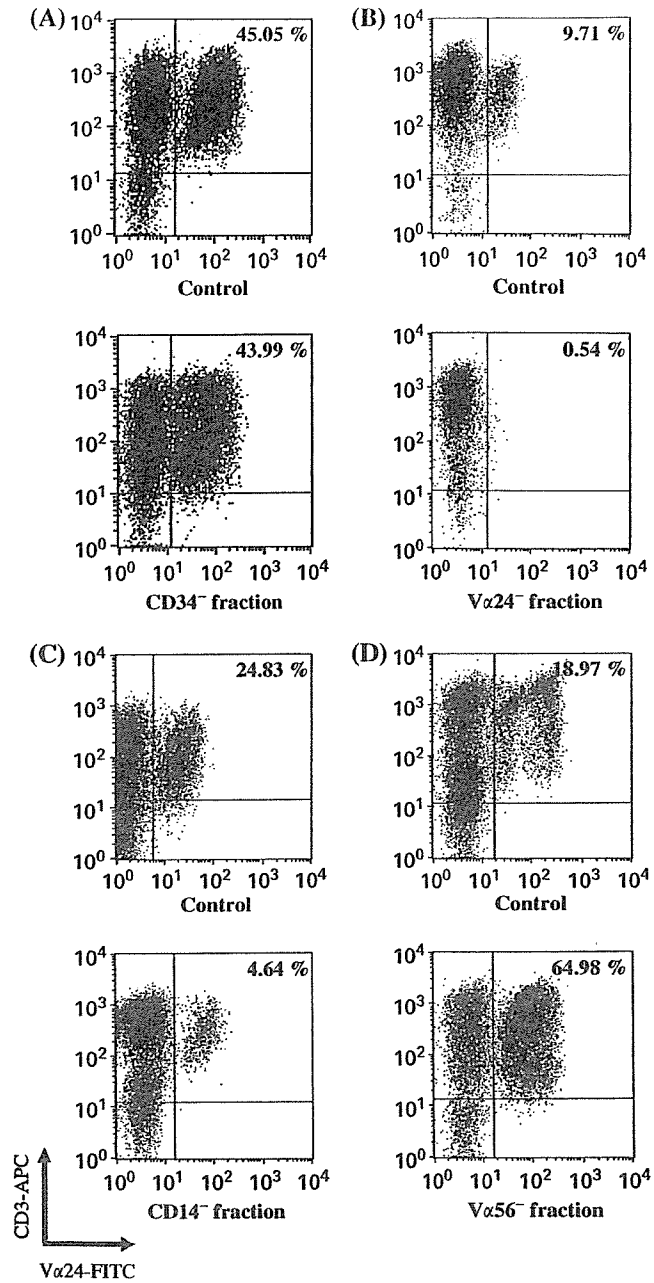

FIGURE 3. Effects of $CD34^+$, $V\alpha24^+$ NKT, $CD14^+$ and $CD56^+$ NK cell depletion on the expansion of $V\alpha24^+$ NKT cells $CD34^+$, $V\alpha24^+$ NKT, $CD14^+$, and $CD56^+$ NK cells were depleted using a MACS sorting system. (A) When $CD34^+$ cells were depleted, $V\alpha24^+$ NKT cells proliferated the same as in culture without $CD34^+$ cell-depletion. When (B) $V\alpha24^+$ NKT cells or (C) $CD14^+$ cells were depleted, $V\alpha24^+$ NKT cells did not expand. (D) When $CD56^+$ NK cells were depleted, the expansion efficiency of $V\alpha24^+$ NKT cells improved. These are each representative results from four experiments. The control in this experiment means the result by using apheresis product without target cell depletion.

treatment, the absolute number of $CD14^+$ cells significantly increased (from 350 ± 81 to $2353 \pm 1220/\mu L$), although their percentage in PB did not change (from 7.24 ± 5.07 to $5.53 \pm 2.10\%$) due to an overwhelming increase in granulocytes. In apheresis products, the proportion of $CD14^+$ cells in nuclear cells also increased 5.7- to 38-fold compared with before G-CSF mobilization, because the apheresis products included low granulocyte contaminations, less than 20%. We obtained $CD14^+$ cells using the MACS system with a purity of $> 95\%$, and made a $CD14^+$ cell gradation (0%, 20%, 40%, 60%, 80% and 100%) under a fixed total cell count of 2.0×10^5 cells/mL/well. The efficacy of $V\alpha24^+$ NKT expansion was related to the initial proportion of $CD14^+$ cells, and the percentage of $V\alpha24^+$ NKT after expansion was increased in $CD14^+$ cell dose dependent manner (Fig. 2B).

Effect of Depletion of Cells, Including $CD34^+$, $V\alpha24^+$ NKT, $CD14^+$ and $CD56^+$ Cells, on $V\alpha24^+$ NKT Cell Expansion

To determine the origin of $V\alpha24^+$ NKT cells and the contribution of each cell population on $V\alpha24^+$ NKT cell expansion, we tested the following cell culture conditions with apheresis products: 1) $CD34^+$ cell-depleted, 2) $V\alpha24^+$ NKT cell-depleted, 3) $CD14^+$ cell-depleted, and 4) $CD56^+$ cell-depleted culture. When $CD34^+$ cells were depleted, $V\alpha24^+$ NKT cells proliferated the same as in non-depleted culture (Fig. 3A). However, the depletion of $V\alpha24^+$ NKT cells completely abrogated the expansion of $V\alpha24^+$ NKT cells (Fig. 3B). Depletion of $CD14^+$ cells also abrogated $V\alpha24^+$ NKT cell expansion to result in the complete disappearance of $V\alpha24^+$ NKT cells on day 12 (Fig. 3C). Interestingly, when $CD56^+$ NK cells were depleted, a remarkable improvement in V $\alpha24^+$ NKT cell proliferation was observed (Fig. 3D). In experiments with $CD56^+$ NK cells separated from $CD56^-$ fraction using a 3.0 μm-pore membrane, the proliferation of $V\alpha24^+$ NKT cells was maintained in $CD56^-$ fractions. The mixed culture of $CD56^+$ NK cells with $CD56^-$ fraction in the same wells resulted in the suppressed proliferation of $V\alpha24^+$ NKT cells, even though there were 1.0×10^5 $CD14^+$ cells (data not shown).

Add-Back of Cells, Including $CD14^+$ Cells, to $V\alpha24^+$ NKT Cell Cultures

The analysis of cell kinetics during culture suggested that $CD14^+$ cells gradually decreased in the early phase (days 0–3), whereas $V\alpha24^+$ NKT cells gradually increased in the latter phase of culture (days 9–12). With regard to $CD56^+$ NK cell kinetics, cell numbers continued to increase during culture in good responders (Fig. 4A), whereas they peaked on day 9 in poor responders (Fig. 4B). To evaluate the effects of $CD14^+$ NK cells in the early phase and late phase of $V\alpha24^+$ NKT cell expansion, we depleted and added back $CD14^+$ cells to the $CD14^-$ cell population, which included $V\alpha24^+$ NKT cells, on

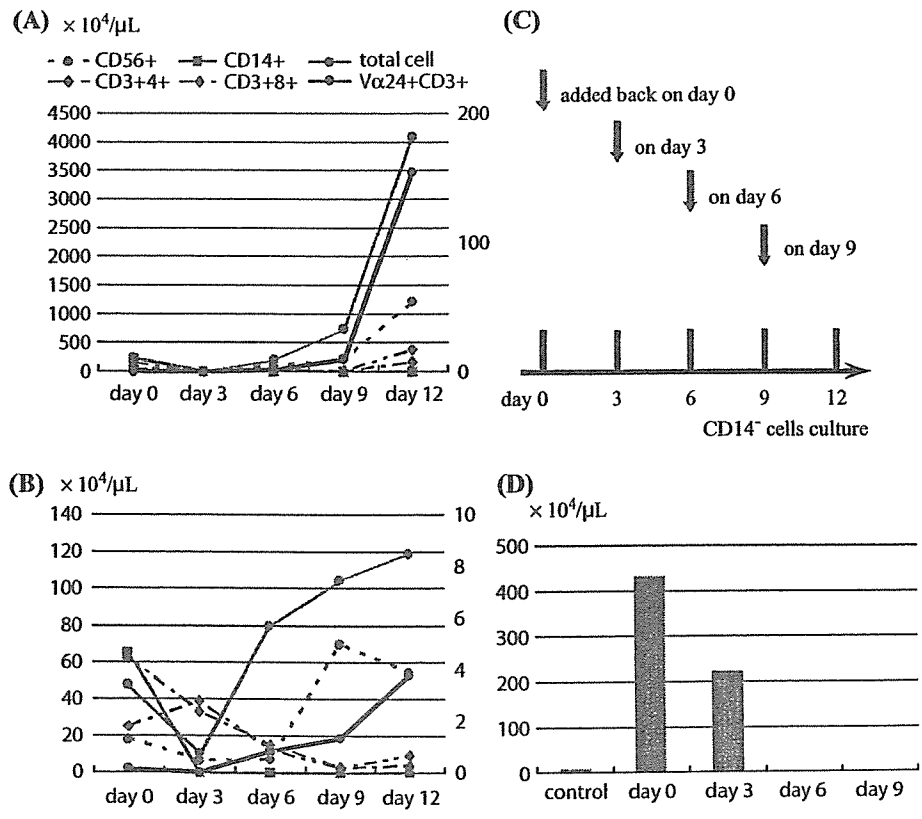

FIGURE 4. Cell kinetics of $V\alpha24^+$ NKT cells and $CD56^+$ NK cells in good and poor expanders (A) In a good-expanding donor, both $CD56^+$ NK cells and $V\alpha24^+$ NKT cells continued to proliferate without decline (representative results from four experiments). The right hand y-axis is used for the cell number of $V\alpha24^+$ NKT cells. (B) In a poor-expanding donor, $CD56^+$ NK cells proliferated more efficiently than $V\alpha24^+$ NKT cells, with a peak on day 9, concomitant with a suppression of $V\alpha24^+$ NKT cell proliferation on day 12 (representative results from four experiments). The right hand y-axis is used for the cell number of $V\alpha24^+$ NKT cells. (C) We added-back $CD14^+$ cells to $CD14^-$ cells on days 0, 3, 6, and 9. (D) Add-back of $CD14^+$ cells before day 3 enhanced the proliferation of $V\alpha24^+$ NKT cells. These are representative results from four independent experiments. All of four experiments were comparable and had a same tendency.

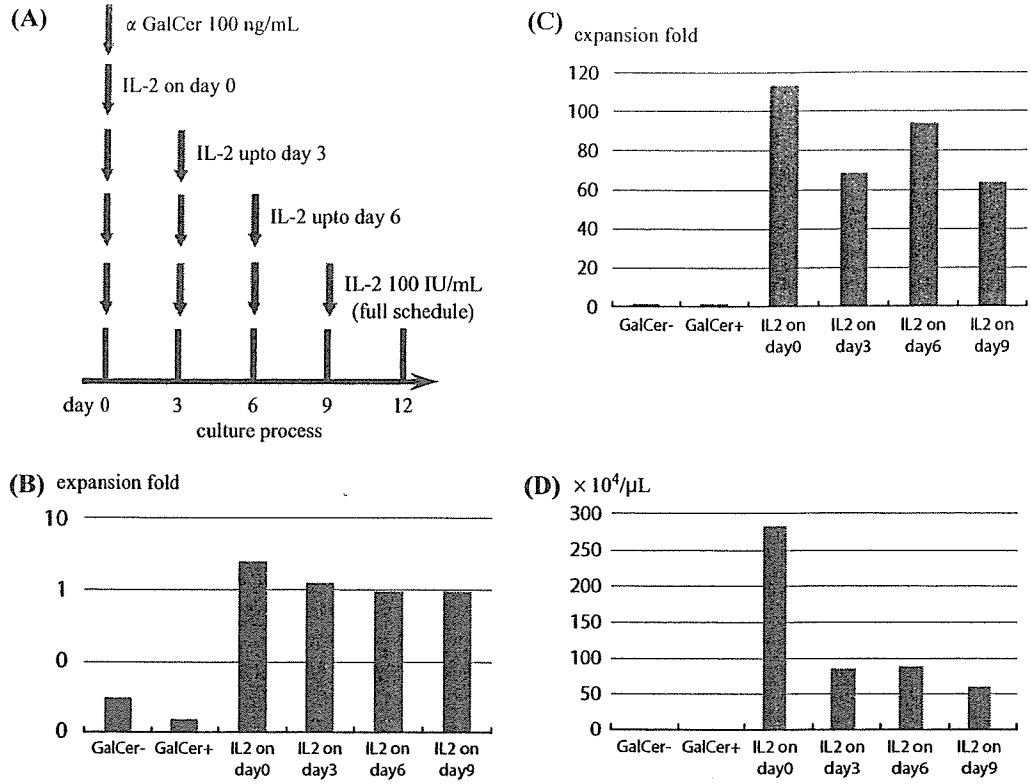

FIGURE 5. Effects of treatment with IL-2 on the expansion of Vα24$^+$ NKT cells (A) We tested different schedules for the administration of IL-2, as follows: on day 0 only, on days 0 and 3, on days 0, 3 and 6, and on days 0, 3, 6 and 9. We found that (B) the expansion-fold of whole cells, and the expansion-fold of the proportion (C) and absolute number (D) of Vα24$^+$ NKT cells were higher when IL-2 was supplemented on day 0 only (representative results from four experiments). All of four experiments were comparable and had a same tendency. In this experiments, α-GalCer was also supplemented at the concentration of 100 ng/mL without non-α-GalCer supplemented control.

days 0, 3, 6 and 9, respectively (Fig. 4C). Figure 4D shows that add-back of CD14$^+$ cells on day 0 induced the highest expansion of Vα24$^+$ NKT cells, whereas the addition of CD14$^+$ cells in the late phase did not show any remarkable benefit.

Effect of IL-2 Supplementation on the Expansion of CD56$^+$ NK Cells and Vα24$^+$ NKT Cells

We hypothesized that repeated IL-2 supplementation could result in the enhancement of CD56$^+$ NK activity to suppress the proliferation of Vα24$^+$ NKT cells.[10] In Figure 5, we tested four different schedules of IL-2 administration: on day 0 only, on days 0 and 3, on days 0, 3 and 6, and on days 0, 3, 6 and 9 (Fig. 5A). We found that whole cells and Vα24$^+$ NKT cells expanded most effectively when IL-2 was added on day 0 only (Figs. 5B–D).

DISCUSSION

The methods that have been used for the ex vivo expansion of human NKT cells can be divided into two categories: simple culture of PBMC with α-GalCer,[11,12] and a two-step culture method that uses α-GalCer-pulsed monocytes as feeder cells.[13–15] A single culture system has the benefit of simplicity and a low risk of contamination, and a major obstacle in a two-step culture system is the availability of a large number of feeder cells. Hence, in this study of the former type, we intended to improve and establish culture conditions for realistic clinical application. Previously, we used a single stimulation of α-GalCer on the initial day, and then administered IL-2 every 3 days to obtain satisfactory expansion of human Vα24$^+$ NKT cells.[7] We have also reported that the addition of 5% autologous plasma was also effective.[8] G-CSF mobilization increased the efficacy of Vα24$^+$ NKT cell expansion, and our data suggested that this was due to a change in cellular component including CD14$^+$ cells[16] and serous factors in the blood. In our present study, we found that CD14$^+$ cells, which are effectively mobilized together with CD34$^+$ cells by G-CSF,[16] are one of the candidates hat contribute to the effective ex vivo expansion of Vα24$^+$ NKT cells. Only the number of pre-cultured CD14$^+$ cells affected the magnitude of the expansion of Vα24$^+$ NKT cells, and this agreed with a

previous report by van der Vliet et al that dendritic cells (DC) derived from monocytes including $CD14^+$ cells could efficiently mediate the expansion of $V\alpha24^+$ NKT cells.[17,18] Additionally, we showed that 1) depletion of $CD14^+$ cells resulted in the loss of $V\alpha24^+$ NKT cell expansion, and 2) the expansion efficacy of $V\alpha24^+$ NKT cells depended on the ratio of $CD14^+$ cells at the initiation of culture. Based on these observations, we speculated that the initial presence of $CD14^+$ cells plays an important role in the subsequent effective expansion of $V\alpha24^+$ NKT cells. We observed that the intensity of CD1d molecules on $CD14^+$ cells, which is critical for interaction with α-GalCer for the expansion of $V\alpha24^+$ NKT cells,[19] increased after G-CSF mobilization (data not shown). Hence, it is reasonable to speculate that more $CD14^+$ cells with a high intensity of CD1d molecules plays a key role in NKT cell expansion. The higher expansion efficiency in apheresis products compared with G-CSF-mobilized PB may be secondary to a higher concentration of $CD14^+$ cells.

The removal of $V\alpha24^+$ NKT cells before culture resulted in the loss of $V\alpha24^+$ NKT cell proliferation, and this supported previous reports that ex vivo-expanded $V\alpha24^+$ NKT cells were neither committed nor supported by $CD34^+$ cells, but were derived from peripheral circulating V α 24^+ NKT cells.[17] Whereas $CD34^+$ cells do not appear to be directly involved in the expansion of $V\alpha24^+$ NKT cells, they might make the circumstances suitable for $V\alpha24^+$ NKT cell expansion, through the secretion of unidentified soluble factors from bone marrow-derived stromal cells, as suggested by Johnston et al.[20] Although the presence of $V\alpha24^+$ NKT cells on day 0 is critical for the expansion of $V\alpha24^+$ NKT cells, no correlation was found between the proportion of $V\alpha24^+$ cells before culture and the proportion of $V\alpha24^+$ NKT cells at the end of culture. This suggests that some other factor(s) might regulate the expansion kinetics of $V\alpha24^+$ NKT cells. The inhibition of cell expansion by $CD56^+$ NK cells was restored when direct cell-to-cell contact was interrupted, which suggests that direct interaction between $V\alpha24^+$ NKT cell and $CD56^+$ NK cells plays a role. This hypothesis was indirectly supported by the phenomina that IL-2 supplementation in every 3 days suppressed expansion of $V\alpha24^+$ NKT cells. Indeed, NK cell-mediated interference of NKT cells is well known to be a primary immune regulatory mechanism.[21] Another possibility is indirect inhibition through the modulation of DC functions. It has been reported that NK cells could yield cytolytic activity against DC during their expansion.[22–24] NKT cells were also activated by DC, resulting in the suppression and killing of DC[25,26] in the same manner as NK cells.

In conclusion, for the efficient ex vivo expansion of $V\alpha24^+$ NKT cells, the presence of $V\alpha24^+$ cells and $CD14^+$ cells at the initiation of culture is critical. NK cells may interact with antigen presenting cells (APC) and interfere with the expansion of NKT cells by hindering the function of antigen presentation or providing direct cytotoxicity against APC. We believe that these findings may be useful for the development of an efficient system for the expansion of NKT cells for future adaptive immunotherapy.

ACKNOWLEDGMENTS

This research was supported by a Grant-in-Aid for Scientific Research from the Ministry of Health, Labour and Welfare of Japan.

REFERENCES

1. Bendelac A, Rivera MN, Park SH, et al. Mouse CD1-specific NK1 T cells: development, specificity, and function. *Annu Rev Immunol.* 1997;15:535–562.
2. Kawano T, Cui J, Koezuka Y, et al. Natural killer-like nonspecific tumor cell lysis mediated by specific ligand-activated Valpha14 NKT cells. *Proc Natl Acad Sci USA.* 1998;95:5690–5693.
3. Kawano T, Cui J, Koezuka Y, et al. CD1d-restricted and TCR-mediated activation of valpha14 NKT cells by glycosylceramides. *Science.* 1997;278:1626–1629.
4. Brossay L, Chioda M, Burdin N, et al. CD1d-mediated recognition of an alpha-galactosylceramide by natural killer T cells is highly conserved through mammalian evolution. *J Exp Med.* 1998; 188:1521–1528.
5. Kobayashi E, Motoki K, Uchida T, et al. KRN7000, a novel immunomodulator, and its antitumor activities. *Oncol Res.* 1995;7:529–534.
6. Toura I, Kawano T, Akutsu Y, et al. Cutting edge: inhibition of experimental tumor metastasis by dendritic cells pulsed with alpha-galactosylceramide. *J Immunol.* 1999;163:2387–2391.
7. Asada-Mikami R, Heike Y, Harada Y, et al. Increased expansion of V alpha 24+ T cells derived from G-CSF-mobilized peripheral blood stem cells as compared to peripheral blood mononuclear cells following alpha-galactosylceramide stimulation. *Cancer Sci.* 2003; 94:383–388.
8. Harada Y, Imataki O, Heike Y, et al. Expansion of α-Galactosylceramide-stimulated Vα24+ NKT cells cultured in the absence of animal materials. *J Immunother.* 2005;28:314–321.
9. Spada FM, Koezuka Y, Porcelli SA. CD1d-restricted recognition of synthetic glycolipid antigens by human natural killer T cells. *J Exp Med.* 1998;188:1529–1534.
10. Mazumder A, Rosenberg SA. Successful immunotherapy of natural killer-resistant established pulmonary melanoma metastases by the intravenous adoptive transfer of syngeneic lymphocytes activated in vitro by interleukin 2. *J Exp Med.* 1984;159:495–507.
11. Van Der Vliet HJ, Nishi N, Koezuka Y, et al. Effects of alpha-galactosylceramide (KRN7000), interleukin-12 and interleukin-7 on phenotype and cytokine profile of human Valpha24+ Vbeta11+ T cells. *Immunology.* 1999;98:557–563.
12. Nicol A, Nieda M, Koezuka Y, et al. Human invariant valpha24+ natural killer T cells activated by alpha-galactosylceramide (KRN7000) have cytotoxic anti-tumour activity through mechanisms distinct from T cells and natural killer cells. *Immunology.* 2000;99:229–234.
13. Kawano T, Nakayama T, Kamada N, et al. Antitumor cytotoxicity mediated by ligand-activated human V alpha24 NKT cells. *Cancer Res.* 1999;59:5102–5105.
14. Nieda M, Nicol A, Koezuka Y, et al. TRAIL expression by activated human CD4(+)V alpha 24NKT cells induces in vitro and in vivo apoptosis of human acute myeloid leukemia cells. *Blood.* 2001;97:2067–2074.
15. Tahir SM, Cheng O, Shaulov A, et al. Loss of IFN-gamma production by invariant NK T cells in advanced cancer. *J Immunol.* 2001;167:4046–4050.
16. Rowley SD, Bensinger WI, Gooley TA, et al. Effect of cell concentration on bone marrow and peripheral blood stem cell cryopreservation. *Blood.* 1994;83:2731–2736.
17. van der Vliet HJ, Nishi N, Koezuka Y, et al. Potent expansion of human natural killer T cells using alpha-galactosylceramide

(KRN7000)-loaded monocyte-derived dendritic cells, cultured in the presence of IL-7 and IL-15. *J Immunol Methods.* 2001;247:61–72.
18. van der Vliet HJ, Molling JW, Nishi N, et al. Polarization of Valpha24+ Vbeta11+ natural killer T cells of healthy volunteers and cancer patients using alpha-galactosylceramide-loaded and environmentally instructed dendritic cells. *Cancer Res.* 2003;63:4101–4106.
19. Nieda M, Nicol A, Koezuka Y, et al. Activation of human Valpha24NKT cells by alpha-glycosylceramide in a CD1d-restricted and Valpha24TCR-mediated manner. *Hum Immunol.* 1999; 60:10–19.
20. Johnston B, Kim CH, Soler D, et al. Differential chemokine responses and homing patterns of murine TCR alpha beta NKT cell subsets. *J Immunol.* 2003;171:2960–2969.
21. Yang OO, Racke FK, Nguyen PT, et al. CD1d on myeloid dendritic cells stimulates cytokine secretion from and cytolytic activity of V alpha 24J alpha Q T cells: a feedback mechanism for immune regulation. *J Immunol.* 2000;165:3756–3762.
22. Chambers BJ, Salcedo M, Ljunggren HG. Triggering of natural killer cells by the costimulatory molecule CD80 (B7-1). *Immunity.* 1996;5:311–317.
23. Wilson JL, Heffler LC, Charo J, et al. Targeting of human dendritic cells by autologous NK cells. *J Immunol.* 1999;163:6365–6370.
24. Pan PY, Gu P, Li Q, et al. Regulation of dendritic cell function by NK cells: mechanisms underlying the synergism in the combination therapy of IL-12 and 4-1BB activation. *J Immunol.* 2004; 172:4779–4789.
25. Nicol A, Nieda M, Koezuka Y, et al. Dendritic cells are targets for human invariant Valpha24+ natural killer T-cell cytotoxic activity: an important immune regulatory function. *Exp Hematol.* 2000; 28:276–282.
26. Nieda M, Kikuchi A, Nicol A, et al. Dendritic cells rapidly undergo apoptosis in vitro following culture with activated CD4+ Valpha24 natural killer T cells expressing CD40L. *Immunology.* 2001;102:137–145.

Allogeneic MHC Gene Transfer Enhances Antitumor Activity of Allogeneic Hematopoietic Stem Cell Transplantation without Exacerbating Graft-versus-Host Disease

Masaki Ohashi,[1,4] Akihiko Kobayashi,[2] Hidehiko Hara,[2] Yoshiaki Miura,[1] Kimiko Yoshida,[1] Miwa Kushida,[2] Yoshinori Ikarashi,[3] Masaki Mandai,[5] Masaki Kitajima,[4] Teruhiko Yoshida,[1] and Kazunori Aoki[2]

Abstract Enhancement of the specific antitumor activity of allogeneic hematopoietic stem cell transplantation (alloHSCT) against solid cancers is a major issue in the clinical oncology. In this study, we examined whether intratumoral allogeneic MHC (alloMHC) gene transfer can enhance the recognition of tumor-associated antigens by donor T cells and augment the antitumor activity of alloHSCT. In minor histocompatibility antigen–mismatched alloHSCT (DBA/2→BALB/c: H-2^d) recipients, alloMHC gene (*H-2K*^{b}) was transduced directly into a s.c. tumor of CT26 colon cancer cells. Because CT26 cells have an aggressive tumorigenicity in syngeneic BALB/c mice, an *H-2K*^{b} gene transfer provides only a limited antitumor effect after syngeneic (BALB/c→BALB/c) HSCT. By contrast, the *H-2K*^{b} gene transfer caused significant tumor suppression in the alloHSCT recipients, and this suppression was evident not only in the gene-transduced tumors but also in simultaneously inoculated distant tumors without gene transduction. *In vitro* cytotoxicity assay showed specific tumor cell lysis by donor T cells responding to the *H-2K*^{b} gene transfer. Graft-versus-host disease was not exacerbated serologically or clinically in the treated mice, demonstrating that alloMHC gene transfer enhances the antitumor effects of alloHSCT without exacerbating graft-versus-host disease. This combination strategy has important implications for the development of therapies for human solid cancers.

Allogeneic hematopoietic stem cell transplantation (alloHSCT) often leads to a significant graft-versus-tumor (GVT) effect, and has proved to be an effective therapeutic approach for several types of leukemia, particularly acute and chronic myelogenous leukemia. Recently, alloHSCT has been applied not only for hematologic malignancies but also for solid cancers, such as renal and breast cancers (1–8). However, the benefit of the GVT effect is often offset by the occurrence of graft-versus-host disease (GVHD), a potentially fatal adverse effect primarily mediated by donor T cells. It is commonly believed that in MHC-matched alloHSCTs, the target antigens for a GVT effect include tumor-associated antigens (TAA) and ubiquitously or tissue-specifically expressed minor histocompatibility antigens (mHA), whereas the targets for GVHD are mHAs. Therefore, efforts to selectively enhance a donor T-cell response to TAAs may provide a means to augment antitumor activity without a concomitant increase in toxicity.

Intratumoral transfer of an allogeneic MHC (alloMHC) gene modifies tumor cells to express the alloMHC molecule, a highly immunogenic antigen that causes an allogeneic rejection response. In the process of this response, cytolytic T lymphocytes are generated not only against the modified tumor cells but also against unmodified tumor cells (9). A putative mechanism for the induction of specific tumor immunity is that the allogeneic response increases local production of cytokines, facilitates antigen presentation and T-cell accumulation, and consequently causes sensitization to previously unrecognized TAAs. Clinical trials with direct intratumoral injection of the human leukocyte antigen-*B7* gene–expressing plasmid DNA complexed with liposome revealed a higher safety profile and systemic response in substantial populations (10-15%) in patients with melanoma and head and neck cancer (10–16). The treatment seemed to be promising but showed a limited clinical efficacy, for which the immune tolerance established between tumor and host may be one of the plausible explanations (17).

We expect that an alloMHC gene transfer could enhance the GVT effect by promoting recognition of TAAs by the donor immune system in alloHSCT recipients, and also that alloHSCT, on the other hand, could augment the therapeutic efficacy of an alloMHC gene transfer by providing a "fresh"

Authors' Affiliations: [1]Genetics Division, [2]Section for Studies on Host-Immune Response, and [3]Pharmacology Division, National Cancer Center Research Institute, [4]Department of Surgery, Keio University School of Medicine Tokyo, Japan, and [5]Department of Obstetrics and Gynecology, Kyoto University Hospital, Kyoto, Japan
Received 12/5/05; revised 1/27/06; accepted 2/2/06.
Grant support: Second and Third Term Comprehensive 10-Year Strategy for Cancer Control from the Ministry of Health, Labour and Welfare of Japan; grants-in-aid for Cancer Research from the Ministry of Health, Labour and Welfare of Japan; and Research Resident Fellowship from the Foundation for Promotion of Cancer Research (M. Ohashi and Y. Miura).
The costs of publication of this article were defrayed in part by the payment of page charges. This article must therefore be hereby marked *advertisement* in accordance with 18 U.S.C. Section 1734 solely to indicate this fact.
Requests for reprints: Kazunori Aoki, Section for Studies on Host-Immune Response, National Cancer Center Research Institute, 5-1-1 Tsukiji, Chuo-ku, 104-0045 Tokyo, Japan. Phone: 81-3-3542-2511; Fax: 81-3-3541-2685; E-mail: kaoki@gan2.res.ncc.go.jp.

doi:10.1158/1078-0432.CCR-05-2657

immune system in which tolerance to tumor cells is not yet induced. In this study, using an MHC ($H\text{-}2^d$)-matched mouse alloHSCT model, we found that an intratumoral alloMHC ($H\text{-}2K^b$) gene transfer significantly enhanced the antitumor effects of alloHSCT against a murine colon cancer. Importantly, GVHD was not exacerbated in any of the treated mice, suggesting the augmentation of tumor-specific immunity of donor T cells by the $H\text{-}2K^b$ gene transfer.

Materials and Methods

Animals and transplantation. Seven- to 9-week-old female BALB/c ($H\text{-}2^d$, Ly-1.2) and DBA/2 ($H\text{-}2^d$, Ly-1.1) mice were purchased from Charles River Japan, Inc. (Kanagawa, Japan) and were housed under sterilized conditions. Nine- to 10-week-old BALB/c mice received a lethal dose (9 Gy) of total body irradiation on the day of transplantation. The irradiated BALB/c mice were injected i.v. with 5×10^6 of T cell–depleted bone marrow cells and 2×10^6 splenic T cells from donor DBA/2 or BALB/c mice in a total volume of 0.2 mL Dulbecco's PBS solution, and the transplanted mice were designated as alloBMT or synBMT, respectively. Bone marrow cells were isolated from donors by flushing each femur and tibia with RPMI 1640 supplemented with 5% heat-inactivated fetal bovine serum (ICN Biomedicals, Inc., Irvine, CA), and splenic cells were prepared by macerating the spleens with a pair of tweezers. After lysis of the erythrocytes, the bone marrow and splenic cells were incubated with anti-Thy-1.2 immunomagnetic beads (Miltenyi Biotec, Bergisch Gladbach, Germany) at 4°C for 15 minutes, followed by depletion and selection of T cells by AutoMACS (Miltenyi Biotec), respectively. More than 90% of T cells were depleted from the bone marrow cells.

Tumor cell lines. CT26 and Renca are weakly immunogenic BALB/c-derived colon and renal cancer cell lines, respectively, and were obtained from the American Type Culture Collection (Rockville, MD). Both cell lines were confirmed to express MHC class I molecules ($H\text{-}2K^d$ and $H\text{-}2D^d$) abundantly by flow cytometry (data not shown). Cells were maintained in RPMI containing 10% fetal bovine serum, 2 mmol/L L-glutamine, and 0.15% sodium bicarbonate (complete RPMI). A CT26 cell line that stably expresses the $H\text{-}2K^b$ gene was generated by retrovirus vector-mediated transduction and designated as CT26/H-$2K^b$.

Fluorescence-activated cell sorting analysis. FITC-conjugated monoclonal antibodies (mAb) to identify mouse H-$2K^b$, CD4, CD8, and phycoerythrin-conjugated mAb to CD3 were purchased from BD PharMingen (San Diego, CA), and FITC-conjugated mAbs to Ly-1.1 and Ly-1.2 were purchased from Meiji Dairies Co. (Tokyo, Japan). Cells were incubated with the relevant mAbs in a total volume of 100 μL PBS with 5% fetal bovine serum for 30 minutes at 4°C. Cells were then washed twice with PBS containing 5% fetal bovine serum, suspended in PBS, and analyzed by FACSCalibur (BD Biosciences, San Jose, CA). Irrelevant IgG mAbs were used as a negative control. Ten thousand live events were acquired for analysis. Allogeneic donor (DBA/2) T-cell engraftment was determined by the percentages of Ly-1.1$^+$ cells among CD3$^+$ cells.

Evaluation of GVHD. The degree of clinical GVHD in transplant recipients was assessed weekly by a scoring system that sums changes in five variables: weight loss, posture, activity, fur texture, and skin integrity (maximum index, 10) as previously described (18). In some recipients, selected serum chemistry was also examined for evaluation of GVHD.

In vitro *cell proliferation assay.* CT26/H-$2K^b$ and CT26 cells were seeded at 2×10^3 per well in 96-well flat plates (Nunc A/S, Roskilde, Denmark). Cell numbers were assessed by a colorimetric cell viability assay using a water-soluble tetrazolium salt (Tetracolor One; Seikagaku Co., Tokyo, Japan) for 4 days after the seeding. The absorbance was determined by spectrophotometry using a wavelength of 450 nm with 595 nm as a reference using ELISA Analyzer (Toyo Sokki, Tokyo, Japan). The assays (carried out in eight wells) were repeated a minimum of twice and the means ± SD were plotted.

In vivo *tumor inoculation and alloMHC gene transfer.* Tumor cells were prepared in a total volume of 50 μL PBS and injected s.c. on the right or left leg. A plasmid DNA expressing the $H\text{-}2K^b$ gene under the control of the Rous sarcoma virus long terminal repeat promotor was used for intratumoral gene transfer. The same vector plasmid DNA without a transgene was used as a negative control. Plasmid DNA-liposome complex per mouse was prepared by addition of 10 μg plasmid DNA into a total of 25 μL PBS, followed by the addition of 25 μL of 0.15 mmol/L DMRIE/DOPE [(+/−)-*N*-(2-hydroxyethyl)-*N*,*N*-dimethyl-2,3-bis(tetradecyloxy)-1-propanaminium bromide/dioleoylphosphatidylethanolamine], which was provided from Vical, Inc. (San Diego, CA). The mixture solution was incubated at room temperature for 15 minutes, and then injected directly into the s.c. tumor. In previous report, presensitization of mice with alloMHC gene–expressing CT26 cells could maximize the therapeutic efficacy of alloMHC gene transfer (9). In this study also, preimmunization with CT26/H-$2K^b$ followed by the treatment with $H\text{-}2K^b$ DNA-liposome complex was done in some of the transplanted mice as an optimized therapeutic control. As a preimmunization treatment, 1×10^6 of 30 Gy–irradiated CT26/H-$2K^b$ cells were i.p. injected twice (at 14 and 7 days) before tumor inoculation. The shortest (r) and longest (l) tumor diameters were measured at indicated days and the tumor volume was determined as $r^2l / 2$. Data are presented as means ± SD.

Cytotoxicity assays. Using 24-well plates (Nunc), responder splenocytes (5×10^6/mL) were cultured with 30 Gy–irradiated CT26/H-$2K^b$ stimulators ($3\text{-}4 \times 10^5$/mL) in a complete RPMI containing 50 μmol/L 2-mercaptoethanol for 5 days. The responder cells were then collected and used as effector cells in a 4-hour chromium release assay against indicated target cells. Concanavalin A lymphoblasts were prepared by stimulating the splenocytes of naïve BALB/c mice for 3 days with 5 μg/mL concanavalin A at 2×10^6/mL in the complete RPMI containing 2-mercaptoethanol. Indicated target cells were labeled by combining 5×10^6 cells with 50 μCi ^{51}Cr (Perkin-Elmer Japan Co., Kanagawa, Japan) in a total volume of 0.2 mL complete RPMI for 1 hour at 37°C, followed by washing thrice with plain RPMI. For the chromium release assay, 5×10^5 effector cells were mixed with 2×10^4 target cells (effector-to-target ratio, 25) in a total volume of 0.2 mL complete RPMI in 96-well round-bottom plates (BD Biosciences). To evaluate the relative contributions of CD4$^+$ and CD8$^+$ T cells to tumor cell lysis, effector cells were incubated with mAb to mouse CD4 (L3L4; PharMingen), CD8 (Ly-2; PharMingen), or both for 30 minutes at 37°C before mixture with target cells. Supernatants were harvested with the Skatron harvesting system (Skatron, Sterling, VA) and counted in a gamma counter (Packard Bioscience Company, Meriden, CT). Percentage of cytotoxicity was calculated as [(experimental cpm − spontaneous cpm) / (maximum cpm − spontaneous cpm)] × 100. Spontaneous cpm was obtained from targets cultured in medium alone, and maximum cpm was obtained from targets incubated in 1% NP40. Each assay was done in triplicate.

In vivo ***depletion of T-cell function.*** To deplete specific immune effector cell subsets before and during treatment with $H\text{-}2K^b$ gene transfer, the transplanted mice received i.p. injections of 0.3 mg mAbs from the anti-CD4$^+$ hybridoma (clone GK1.5, rat IgG_{2b}) and/or anti-CD8$^+$ hybridoma (clone Lyt-2.1, mouse IgG_{2b}; ref. 19). Injections started 5 days before the inoculation with CT26 cells and the treatment repeated every 5 to 6 days throughout the entire experimental period to ensure depletion of the targeted cell type. CD4$^+$ and CD8$^+$ T-cell depletion was confirmed by flow cytometry of splenic suspensions at the time of tumor injection and weekly afterward.

Statistical analysis. Comparative analyses of the data were done by the Student's t test using SPSS statistical software (SPSS Japan, Inc., Tokyo, Japan). $P < 0.05$ was considered as a significant difference.

Results

AlloHSCT causes GVHD and GVT effects. We first assessed the posttransplant immune reconstitution of T cells and donor chimerism of splenic $CD3^+$ T cells in alloBMT recipients (DBA/2→BALB/c). To exclude biases related to transplant procedures, including lethal irradiation, we conducted synBMT (BALB/c→BALB/c) as a control. The reconstitution of both $CD4^+$ and $CD8^+$ T cells was delayed in alloBMT recipients compared with that in synBMT recipients at 8 weeks posttransplantation (Fig. 1A), which was consistent with other reports (20–22). The early (≤2 weeks) posttransplant mortality, most likely due to acute GVHD or graft failure, was usually <15% in transplant recipients. Analysis of donor engraftment showed 95.7 ± 1.5% donor type in alloBMT recipients (n = 3) at 8 weeks posttransplantation.

We then examined whether our alloHSCT models generate any GVHD and GVT effects. The clinical score of GVHD severity at 8 weeks was ~4 in alloBMT recipients, whereas it was <1 in synBMT recipients (Fig. 1B). Death from GVHD was rarely observed during the first 3 months after the transplantation. For evaluation of GVT effects, 1×10^6 CT26 or 2×10^6 Renca cells were s.c. inoculated into the mice 8 to 9 weeks posttransplantation. The growth of the tumors was substantially, although not statistically significantly, suppressed in the alloBMT recipients compared with that in the synBMT recipients (Fig. 1C). Our alloHSCT model was shown to constantly cause GVHD and a limited but detectable level of the GVT effect, which is highly similar to a clinical setting after allogeneic HSCT.

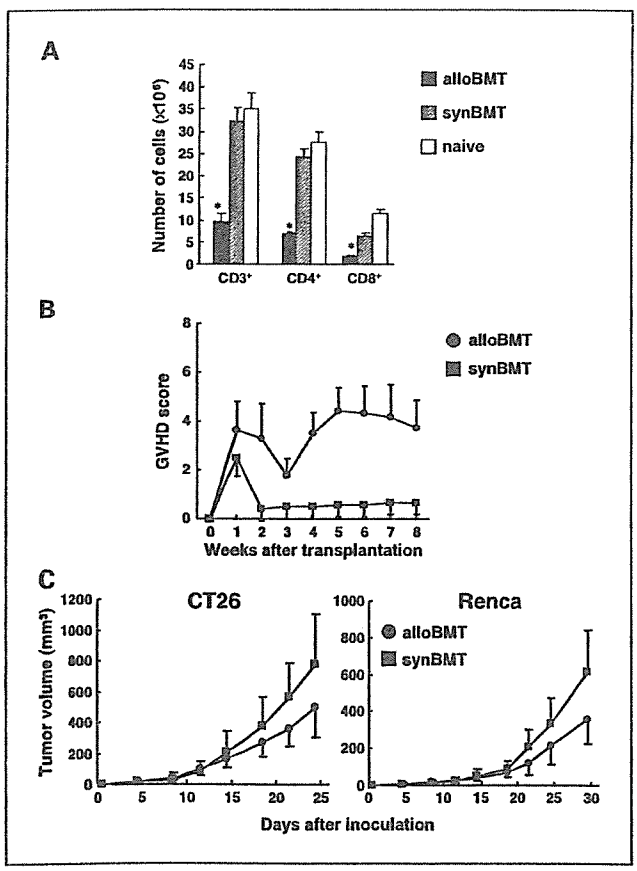

Fig. 1. Clinical GVHD score and s.c. tumor growth in alloBMT or synBMT recipients. *A*, T-cell immune reconstitution in alloBMT or synBMT mice. The absolute number of splenic T cells was measured 8 weeks after the transplantation (n = 3 per group). *, $P < 0.05$ compared with synBMT. *B*, clinical course of GVHD in the recipient mice. Clinical GVHD scores were assessed weekly after the transplantation by a scoring system that sums changes in five clinical variables as described in the text (maximum index, 10; synBMT, n = 13; alloBMT, n = 11). *C*, growth curves of CT26 and Renca s.c. tumors in the recipient mice. Eight weeks after the transplantation, CT26 and Renca cells were inoculated s.c. and tumor sizes were measured on the days indicated (n = 4–6 per group). Representative of at least three independent experiments.

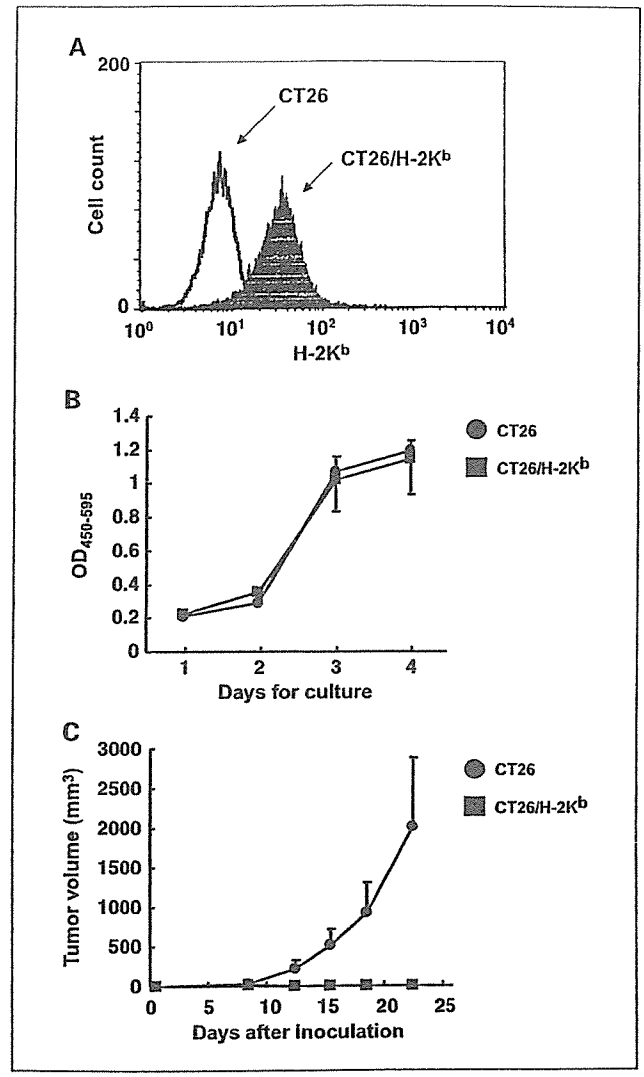

Fig. 2. Immune rejection of CT26/H-$2K^b$ cell line in BALB/c mice. *A*, flow cytometric analysis of CT26/H-$2K^b$ and unmodified CT26 cells. Cells were incubated with FITC-conjugated antibody to mouse H-$2K^b$ and flow cytometry was carried out by FACSCalibur. *B, in vitro* cell proliferation assay. Number of CT26 and CT26/H-$2K^b$ cells was assessed by a colorimetric cell viability assay. Each assay was done in eight wells. $OD_{450\text{-}595}$, absorbance at 450 to 595 nm. *C, in vivo* rejection of CT26/H-$2K^b$ tumors. CT26 and CT26/H-$2K^b$ cells were injected s.c. into the legs of naive BALB/c mice and tumor sizes were measured on the days indicated (n = 5 per group).

AlloMHC gene–transduced tumor cells cause an immune response in vivo. To determine whether alloMHC gene–transduced CT26 cells could induce an immune response in

mice, the tumorigenicity of CT26/H-2K^b cells was compared with that of unmodified CT26 cells. Flow cytometric analysis confirmed the expression of the H-2K^b molecule in CT26/H-2K^b cells (Fig. 2A), and the *in vitro* proliferation of CT26/H-2K^b cells was compatible with that of unmodified CT26 cells (Fig. 2B). However, when injected s.c. into naïve BALB/c mice, CT26/H-2K^b cells did not form a tumor mass over 3 weeks (n = 5), whereas unmodified CT26 cells developed a rapidly growing tumor during the same period (n = 5; Fig. 2C), suggesting that the alloMHC gene-transduced tumor cells are highly antigenic and cause an immune response *in vivo*. No apparent toxicity was observed in the CT26/H-2K^b cell-inoculated mice.

AlloMHC gene transfer induces synergistic antitumor effect with alloHSCT. To examine whether alloMHC gene transfer could enhance the antitumor effects of alloHSCT, the mice were inoculated s.c. with 1 × 10^6 CT26 cells at 8 weeks posttransplantation, and *H-2K^b* gene-expressing plasmid DNA complexed with liposome was injected into the tumor thrice (at 5, 7, and 9 days) after the inoculation. The tumor volumes at day 5 were ~60 to 100 mm^3. Preimmunization with irradiated CT26/H-2K^b cells was carried out in a group of transplanted mice as a positive control to maximize the effect of the *H-2K^b* immune gene therapy (9). A single injection of plasmid DNA-liposome complexes showed ~1% gene transduction efficiency *in vivo* (data not shown). The control empty vector was not immunogenic *in vivo* because the tumor volume of the negative control group without any intratumoral injections was similar to that of the empty plasmid-injected group (Fig. 3A). In the CT26/H-2K^b-preimmunized mice, *H-2K^b* gene transfer caused significant tumor suppression after either type of transplantation, synBMT or alloBMT (Fig. 3A). In non-preimmunized mice, *H-2K^b* gene transfer showed only a limited suppressive effect in synBMT recipients, which was probably due to the aggressive tumorigenicity of CT26 cells *in vivo*, whereas significant suppression of tumor growths was recognized in alloBMT recipients (Fig. 3A). The results showed that alloMHC gene transfer can augment the antitumor effects of donor immune cells in the context of alloHSCT.

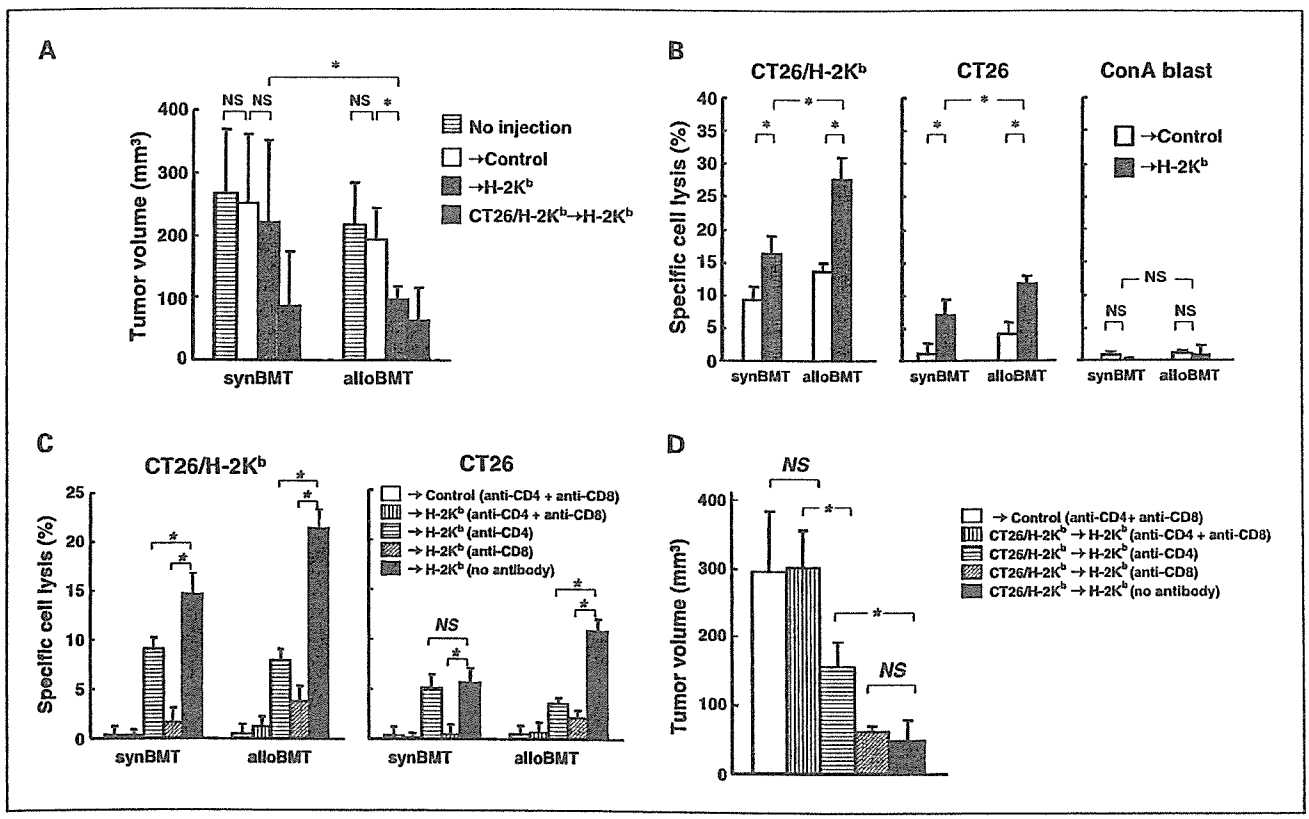

Fig. 3. Synergistic antitumor effect of alloMHC gene transfer in alloBMT recipients. *A*, growth of CT26 s.c. tumors injected with *H-2K^b* vector in alloBMT or synBMT recipients. Eight weeks after the transplantation, CT26 cells were s.c. inoculated and then *H-2K^b* vector or control vector was injected into the tumors thrice. Tumor volume was compared between the groups at 11 days after the completion of vector injection (n = 5-7 per group). As a preimmunization treatment, irradiated CT26/H-2K^b cells were i.p. injected twice before tumor inoculation to maximize the therapeutic efficacy of *H-2K^b* gene transfer. →Control, injection of an empty vector without a transgene. CT26/H-2K^b→H-2K^b, *H-2K^b* gene transfer with preimmunization; →H-2K^b, *H-2K^b* gene transfer without preimmunization. *, $P < 0.05$. NS, not significant. Representative of at least three independent experiments. *B, in vitro* cytotoxicity assay of *H-2K^b*-vector injected mice. Splenocytes were collected from alloBMT or synBMT mice (n = 3-4 per group) 15 days after the completion of vector injection, and their cytotoxicity was evaluated in a standard 4-hour ^{51}Cr release assay (effector/target ratio, 25) against CT26/H-2K^b, CT26 cells, and BALB/c-derived concanavalin A (*ConA*) lymphoblasts after stimulation with irradiated CT26/H-2K^b cells. *, $P < 0.05$ compared with synBMT. *C*, blocking assay of *in vitro* cytotoxicity. Splenocytes from *H-2K^b* gene-transduced alloBMT or synBMT recipients were analyzed for their cytotoxicity in a standard 4-hour ^{51}Cr release assay (effector/target ratio, 25) against CT26/H-2K^b or CT26 cells with anti-CD4 and/or anti-CD8 antibodies. *, $P < 0.05$. *D*, antitumor effect of *H-2K^b* gene transfer in alloBMT recipients after the *in vivo* depletion of CD4$^+$ and CD8$^+$ T cells. Groups of alloBMT mice were treated with anti-CD4 and/or anti-CD8 antibodies to deplete these cell populations, and the CT26 s.c. tumor was injected with *H-2K^b* vector thrice. Tumor volume was compared between the treatment groups at 11 days after the completion of vector injection (n = 6-8). *, $P < 0.05$.

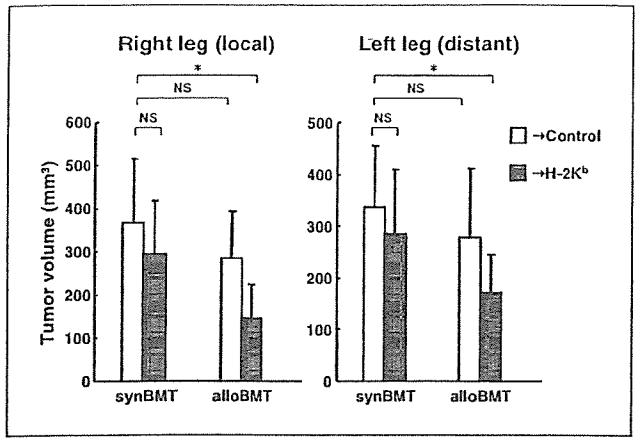

Fig. 4. Suppression of tumors at distant sites by the intratumoral injection of *H-2K*^{b} vector in alloBMT mice. CT26 cells were s.c. inoculated on both legs of alloBMT or synBMT recipients, and H-2K^b vector were injected into only the right leg tumor thrice without preimmunization. Tumor volume at each leg was compared between the treatment groups at 12 days after the completion of vector injection (n = 7-11). *, $P < 0.05$. NS, not significant. Representative of at least three independent experiments.

In vitro cytotoxicity assay was done to assess antitumor cytolytic T-lymphocyte responses induced by alloMHC gene transfer in the non-preimmunized mice. The splenocytes derived from mice bearing *H-2K*^{b}-transduced tumors recognized and lysed unmodified CT26 cells as well as CT26/H-2K^b cells but not concanavalin A blasts, and the cytotoxic activity was higher in the alloBMT recipients than in the synBMT recipients (Fig. 3B). Splenocytes showed higher cytolytic response to CT26/H-2K^b than to CT26 cells, indicating the donor T cells recognize the H-2K^b molecule as an allogeneic antigen.

Both CD4$^+$ and CD8$^+$ T cells contribute to the antitumor immunity. Then, in the *in vitro* blocking assays of lymphocyte cytotoxicity with antimurine CD4 and CD8 antibodies, CD8$^+$ T cells were shown to be the dominant effector in synBMT recipients, whereas both CD4$^+$ and CD8$^+$ T cells were apparently contributive to tumor cell lysis in alloBMT recipients (Fig. 3C).

To further explore the role of CD4$^+$ and CD8$^+$ T cells in antitumor immunity, the preimmunized alloBMT mice were treated with anti-CD4 or anti-CD8 antibodies to deplete these cell populations *in vivo*. The antitumor effect of *H-2K*^{b} gene transfer was completely cancelled in the transplanted mice with depletion of both CD4$^+$ and CD8$^+$ T cells, whereas the animals depleted of CD4$^+$ or CD8$^+$ T cells showed significant tumor growth inhibition (Fig. 3D). This *in vivo* depletion study indicated that the CD4$^+$ and CD8$^+$ cytotoxic T cells play central roles in the generation of antitumor immunity. Whereas CD8$^+$ T cells were more contributive to *in vitro* tumor cell lysis than CD4$^+$ T cells in the *in vitro* cytotoxicity assay (Fig. 3C), CD4$^+$ T cells might be more contributive to *in vivo* tumor inhibition than CD8$^+$ T cells (Fig. 3D). One possible explanation is that CD4$^+$ T cells play a variety of roles *in vivo*, which include enhancement of cellular immunity by interacting with antigen-presenting cells and maintenance of immune memory, as well as direct cytotoxicity. The reason that tumor inhibition in mice depleted of only CD8$^+$ T cells was compatible with that in mice without any T-cell depletion might be that the antitumor effect induced by the cooperative effect of CD4$^+$ and CD8$^+$ cytotoxic T cells was already saturated in the CT26 xenograft model.

AlloMHC gene transfer causes growth suppression of both local and distant tumors in alloHSCT recipients. Next, to evaluate the therapeutic efficacy of alloMHC gene transfer for tumors at distant sites, transplant recipients were s.c. inoculated with 1×10^6 CT26 cells on the right leg and, 5 days later, inoculated with 5×10^5 CT26 cells on the left leg. On the right leg, tumor was then transduced with *H-2K*^{b} gene thrice. In alloHSCT recipients, significant tumor suppression of the treated tumor on the right leg and the untreated tumor on the opposite leg was observed (Fig. 4), which showed that alloMHC gene transfer causes a systemic antitumor immunity in alloHSCT recipients.

Presence of tumor cells at the time of transplantation does not reduce therapeutic efficacy of alloMHC gene transfer. In these experiments, the recipient immune system was reconstituted in the absence of any tumor. To simulate a clinical situation in which patients have residual tumors at the time of alloHSCT, we injected 1×10^6 of 200 Gy–irradiated CT26 cells i.p. into alloBMT recipients at the time of transplantation (day 0) and also at 7 and 14 days posttransplantation. The mice were inoculated with 1×10^6 wild-type CT26 cells at 8 weeks after the transplantation and then injected with *H-2K*^{b} plasmid complexed with liposome. It was conceivable that, in this condition, the donor-derived immune system might acquire tolerance to TAAs during its reconstitution. Nonetheless, *H-2K*^{b} gene transfer, either with or without exposure to wild-type CT26 cells, still led to significant tumor suppression (Fig. 5), indicating that, at least in this HSCT model, the presence of tumor cells at the time of transplantation does not induce immune tolerance to tumor cells and thus does not reduce the efficacy of subsequent alloMHC gene transfer.

AlloMHC gene transfer does not exacerbate GVHD. Although the *in vitro* cytotoxicity assay showed induction of a tumor-specific cytolytic T-lymphocyte response by *H-2K*^{b} gene transfer, alloMHC expression in tumor cells could theoretically promote a donor T-cell response not only against TAAs but also against mHAs shared by tumor and normal cells, which might result in GVHD exacerbation. We thus examined serum chemistry and the clinical GVHD score in the transplanted mice with the *H-2K*^{b} gene transfer. Albumin, total bilirubin, aspartate

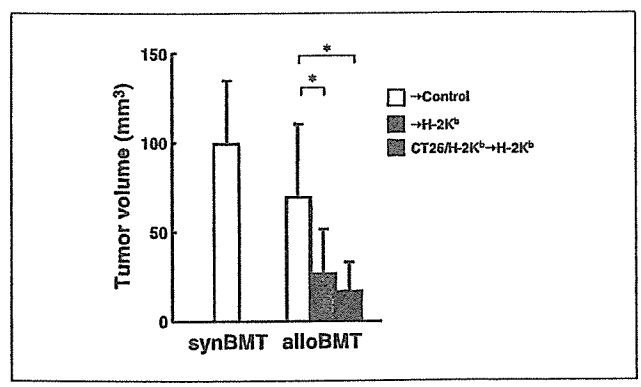

Fig. 5. Preservation of antitumor activity of *H-2K*^{b} gene transfer in alloBMT recipients with tumor present during the immune reconstitution. Irradiated CT26 cells were i.p. injected at the time of transplantation, and 8 weeks after the transplantation the CT26 s.c. tumor was injected with *H-2K*^{b} vector thrice in alloBMT recipients. Tumor volume was compared between the groups at 11 days after the completion of vector injection (n = 6-8). *, $P < 0.05$.

Table 1. Selected serum chemistry and clinical GVHD score

	CT26/H-2K^b→H-2K^b	→H-2K^b	→Control	*P*	Normal
AlloBMT					
Serum					
ALB (g/dL)	3.04 ± 0.22	3.2 ± 0.14	3.06 ± 0.28	NS	2.95 ± 0.23
TB (mg/dL)	0.052 ± 0.03	0.036 ± 0.009	0.05 ± 0.014	NS	0.06 ± 0.01
AST (IU/L)	239 ± 47	269 ± 56	314 ± 83	NS	81 ± 11
ALT (IU/L)	153 ± 33	177 ± 43	171 ± 52	NS	41 ± 14
ALP (IU/L)	428 ± 140	448 ± 110	397 ± 93	NS	365 ± 46
GVHD score	5.6 ± 0.5	5.4 ± 0.5	5.4 ± 0.9	NS	
SynBMT					
Serum					
ALB (g/dL)	3 ± 0.32	3.02 ± 0.25	2.92 ± 0.11	NS	
TB (mg/dL)	0.068 ± 0.023	0.046 ± 0.019	0.04 ± 0.024	NS	
AST (IU/L)	210 ± 34	163 ± 57	213 ± 43	NS	
ALT (IU/L)	88 ± 32	94 ± 44	110 ± 38	NS	
ALP (IU/L)	267 ± 95	286 ± 60	295 ± 86	NS	
GVHD score	2.2 ± 0.8	2 ± 0.7	2.2 ± 0.8	NS	

NOTE: *H-2K^b*-expressing or control vector was intratumorally injected thrice in alloBMT or synBMT recipients with or without preimmunization, and 15 days later the serum chemistry and clinical GVHD score were evaluated (n = 5 per group). "CT26/H-2K^b→H-2K^b" and "→H-2K^b" indicate *H-2K^b* gene transfer with and without preimmunization, respectively.
Abbreviations: ALB, albumin; TB, total bilirubin; AST, aspartate aminotransferase; ALT, alanine aminotransferase; ALP, alkaline phosphatase; NS, not significant.

aminotransferase, alanine aminotransferase, and alkaline phosphatase are the potential indicators of GVHD-related injury of the hepatobiliary system. GVHD was not serologically nor clinically exacerbated in the *H-2K^b* gene-transduced mice compared with the control vector-injected mice (Table 1).

Intratumoral alloMHC gene transfer might, to some extent, cause the gene transduction into normal cells surrounding the tumor cells. To assess its potential toxicity, 10 μg *H-2K^b*-expressing plasmid DNA complexed with liposome was injected thrice into the s.c. space of non-tumor-bearing alloBMT recipients. Mice were then examined for serum chemistry, clinical GVHD score, and histopathology of the skin, liver, and gut 7 days after the vector injection. All of the mice s.c. injected with *H-2K^b* plasmid did not show any significant exacerbation of GVHD (data not shown).

Tumor-specific immunity induced by alloMHC gene transfer is long-lasting in vivo. The CT26 s.c. tumors disappeared in ~10% to 20% of alloBMT mice by alloMHC gene transfer. To examine *in vivo* longevity of the tumor-specific immunity, a total of 11 alloBMT recipients who survived the initial CT26 challenge with complete tumor remission by *H-2K^b* gene transfer were again inoculated with CT26 cells on the right leg and Renca cells on the left leg. Of the 11 mice, eight had been i.p. injected with irradiated CT26 cells at the time of transplantation and three had not. Renca cells formed a tumor mass in all the mice, whereas CT26 cells were rejected in 10 of 11 mice (91%; Table 2), suggesting that TAAs and/or tissue-restricted mHAs are different between CT26 and Renca cells and that the *H-2K^b* gene transfer to CT26 cells increases the recognition of CT26-specific antigens by donor T cells. *In vitro* cytotoxicity assay also showed lysis of CT26 but not Renca cells or concanavalin A lymphoblasts (data not shown). The results showed that the tumor-specific immunity induced by alloMHC gene transfer is potentially long lasting in HSCT recipients.

Discussion

Several experimental investigations have been made thus far to separate a desirable GVT effect for hematologic or solid malignancies from an undesirable GVHD in alloHSCT recipients. Delayed donor leukocyte infusions into the recipients with mixed chimerism (23, 24), expansion and reinfusion of GVT-specific donor T-cell clones (25, 26), posttransplant immunization of the recipients with tumor cell vaccines (27–29), and pretransplant tumor antigen-specific immunization of the donors (30) were reported to have the potential to selectively enhance the GVT effect. On the other hand, administration of interleukin-11 (31), infusion of CD4$^+$CD25$^+$ regulatory T cells (32, 33), blockade of the function of donor antigen-presenting cells (34), and blockade of the GVHD-specific cytotoxic pathway (Fas-Fas ligand or perforin-granzyme; ref. 35) were shown to be capable of preventing GVHD

Table 2. Tumorigenicity of CT26 and Renca cells in alloBMT recipients cured of initial CT26 challenge

Exposure of CT26 cells	Tumor formation	
	CT26 (right leg)	Renca (left leg)
+	1/8	8/8
−	0/3	3/3
Total	1/11 (9%)	11/11 (100%)

NOTE: Eleven alloBMT recipients who survived the initial CT26 challenge with complete tumor remission by *H-2K^b* gene transfer were again inoculated with CT26 cells and Renca cells. Of the 11 mice, eight had been i.p. injected with irradiated CT26 cells at the time of transplantation and three had not.

while maintaining a GVT effect. In the present study, we showed that intratumoral alloMHC gene transfer could enhance the GVT effect without exacerbating GVHD by inducing systemic tumor-specific immunity in MHC-matched alloHSCT recipients.

Although there have been several animal studies showing the potential efficacy of a combination of alloHSCT and gene-based immunotherapy, such as a tumor vaccine using *granulocyte macrophage colony-stimulating factor* and *interleukin 2/herpes simplex thymidine kinase* genes (27–29), the reports only showed that the antitumor immune activity of tumor vaccines could be reproduced in the context of allogeneic transplantation. To our knowledge, ours is the first report that showed a synergistic antitumor effect of immune gene therapy combined with alloHSCT.

The mechanism for the synergism is yet unclear, but a mixed allogeneic and rejection reactions induced by the combination therapy may be of major importance in creating an environment strongly supporting the activation of an antitumor response. Although the recognition of tumor antigens by donor T cells was not strong enough to induce a significant antitumor immune response in the mice treated with alloHSCT alone, the combination with the alloMHC gene transfer may enhance (*a*) trafficking of immune cells into the tumor, (*b*) local production of various cytokines at the tumor site, and (*c*) presentation of tumor antigenic peptides on antigen-presenting cells through uptake of apoptotic tumor cell bodies induced by the alloMHC gene expression. These effects may facilitate the increased recognition of previously unrecognized or weakly recognized tumor antigens by donor T cells, which leads to a significant tumor specific immunity (36, 37). Furthermore, several murine bone marrow transplantation models have shown that $CD4^+$ and $CD8^+$ T cells both contributed to GVHD through their cytolytic activity (31, 38, 39), and in this study also, although the $CD8^+$ T cells seemed to be major effectors of antitumor immunity by the *H-2K*^{b} gene transfer in naïve and synBMT mice (Fig. 3C; ref. 9), the combination of alloHSCT and alloMHC gene transfer was able to induce effective cooperation of $CD4^+$ and $CD8^+$ cytotoxic T cells in tumor cell killing (Fig. 3C and D). The $CD4^+$ T cells may have an important role in the antitumor immunity as well as GVHD in allogeneic HSCT.

In this study, the tumor cells were inoculated into the mice 8 weeks after the transplantation because the CT26 cell–injected BALB/c mice could not survive >2 months due to the aggressive tumorigenicity of the cell. On the other hand, we need at least a 6-week interval between alloHSCT and the immune therapy to allow a sufficient immune reconstitution necessary for the evaluation of the immune therapy. This experiment model does not exactly replicate the clinical situations in which the recipients usually harbor the relapse or residual cancer cells at the time of HSCT, and one could argue that the immune reconstitution in the presence of tumor cells might induce the acquisition of tolerance to tumor antigens. Therefore, we injected the irradiated CT26 cells at the initial phase after transplantation, and confirmed that the *H-2K*^{b} gene transfer elicited effective tumor suppression even in the HSCT recipients exposed to tumor cells during immune reconstitution, suggesting that the alloMHC gene transfer with alloHSCT is a promising therapeutic strategy in clinical setting. As a next step, a combination with other approaches, such as donor lymphocyte infusion and preimmunization with an alloMHC gene–expressing plasmid, might be examined for whether they can further enhance the antitumor effects of alloMHC gene transfer with alloHSCT.

The expression of alloMHC in tumor cells could theoretically promote a donor T-cell response not only for TAAs but also for mHAs shared by tumor and normal host cells, which may cause GVHD. However, in our study, the alloMHC gene transfer did not exacerbate serum enzymes and clinical GVHD scores in alloHSCT recipients. It is possible that much of the immune response was directed against nonimmunodominant mHAs with restricted tissue distribution or possibly even against TAAs, not against immunodominant mHAs. Other reports have also shown that immunization of alloHSCT recipients with a tumor cell vaccine substantially increased GVT activity of donor lymphocytes without exacerbating GVHD (27–30). Luznik et al. hypothesized that the immunogeneic antigen-presenting cells at the vaccine site capture both TAAs and mHAs from tumor cells and promote tumor-specific immunity and GVHD, whereas away from the vaccine site, resting host antigen-presenting cells presenting mHAs induce tolerance in or exhaust alloreactive donor T cells (29, 40). Alloreactive T cells that have been activated at the vaccine site may subsequently become unresponsive to the immunodominant mHAs following an encounter with resting host antigen-presenting cells, whereas tumor-specific T cells would be expected to persist in activated or long-lived memory states. Another possible explanation for the GVT preference over GVHD might be that a major part of potential immunogenic antigens on CT26 tumor cells is TAAs, and indeed it was reported that CT26 cells express high levels of an H-$2L^d$-restricted peptide (AH1) from an endogenous retrovirus, and induce a robust AH-1-specific T-cell response (29, 41). Although we have shown an advantage and safety of the combination therapy in the preclinical study, CT26 cells may not be representative of all clinical human cancers and the occurrence or exacerbation of GVHD should be evaluated carefully in the future stage of the therapeutic development in a clinical study.

Because myeloablative conditioning is associated with a considerable risk of morbidity and mortality and because solid tumors, such as renal cancer, are typically refractory to chemotherapy, the nonmyeloablative alloHSCT is clinically applied against solid tumors (1, 2, 4). Nonmyeloablative alloHSCT often results in a mixed T-cell chimerism, and a donor leukocyte infusion is done for patients with mixed chimerism to achieve exclusively donor-derived hematopoiesis because the establishment of a complete donor chimerism is considered to be crucial for drawing the optimal GVT effect (42, 43). In this study, we used a myeloablative conditioning model to constantly achieve the full donor chimerism, because our primary purpose was to determine the effect of the immune gene therapy on alloHSCT and the full-blown effect after alloHSCT (i.e., complete chimerism). In the clinical setting, the nonmyeloablative conditioning may be optimal to test the potential of the combination therapy to reduce the regimen-related toxicity.

Acknowledgments

We thank Dr. Gary J. Nabel (Vaccine Research Center, National Institutes of Health, Bethesda, MD) for providing the *H-2K*^{b} expression plasmid and for useful discussions, Tomomi Ikeda for technical support, and Vical Incorporated for providing the liposome DMRIE/DOPE.

References

1. Childs R, Chernoff A, Contentin N, et al. Regression of metastatic renal-cell carcinoma after nonmyeloablative allogeneic peripheral-blood stem-cell transplantation. N Engl J Med 2000;343:750–8.
2. Ueno NT, Cheng YC, Rondon G, et al. Rapid induction of complete donor chimerism by the use of a reduced-intensity conditioning regimen composed of fludarabine and melphalan in allogeneic stem cell transplantation for metastatic solid tumors. Blood 2003;102:3829–36.
3. Bishop MR, Fowler DH, Marchigiani D, et al. Allogeneic lymphocytes induce tumor regression of advanced metastatic breast cancer. J Clin Oncol 2004; 22:3886–92.
4. Kanda Y, Komatsu Y, Akahane M, et al. Graft-versus-tumor effect against advanced pancreatic cancer after allogeneic reduced-intensity stem cell transplantation. Transplantation 2005;79:821–7.
5. Bay JO, Fleury J, Choufi B, et al. Allogeneic hematopoietic stem cell transplantation in ovarian carcinoma: results of five patients. Bone Marrow Transplant 2002; 30:95–102.
6. Kurokawa T, Fischer K, Bertz H, Hoegerle S, Finke J, Mackensen A. *In vitro* and *in vivo* characterization of graft-versus-tumor responses in melanoma patients after allogeneic peripheral blood stem cell transplantation. Int J Cancer 2002;101:52–60.
7. Moscardo F, Martinez JA, Sanz GF, et al. Graft-versus-tumour effect in non-small-cell lung cancer after allogeneic peripheral blood stem cell transplantation. Br J Haematol 2000;111:708–10.
8. Zetterquist H, Hentschke P, Thorne A, et al. A graft-versus-colonic cancer effect of allogeneic stem cell transplantation. Bone Marrow Transplant 2001;28: 1161–6.
9. Plautz GE, Yang ZY, Wu BY, Gao X, Huang L, Nabel GJ. Immunotherapy of malignancy by *in vivo* gene transfer into tumors. Proc Natl Acad Sci U S A 1993; 90:4645–9.
10. Nabel GJ, Nabel EG, Yang ZY, et al. Direct gene transfer with DNA-liposome complexes in melanoma: expression, biologic activity, and lack of toxicity in humans. Proc Natl Acad Sci U S A 1993;90:11307–11.
11. Nabel GJ, Gordon D, Bishop DK, et al. Immune response in human melanoma after transfer of an allogeneic class I major histocompatibility complex gene with DNA-liposome complexes. Proc Natl Acad Sci U S A 1996;93:15388–93.
12. Stopeck AT, Jones A, Hersh EM, et al. Phase II study of direct intralesional gene transfer of allovectin-7, an HLA-B7/β_2-microglobulin DNA-liposome complex, in patients with metastatic melanoma. Clin Cancer Res 2001;7:2285–91.
13. Rini BI, Selk LM, Vogelzang NJ. Phase I study of direct intralesional gene transfer of HLA-B7 into metastatic renal carcinoma lesions. Clin Cancer Res 1999;5: 2766–72.
14. Rubin J, Galanis E, Pitot HC, et al. Phase I study of immunotherapy of hepatic metastases of colorectal carcinoma by direct gene transfer of an allogeneic histocompatibility antigen, HLA-B7. Gene Ther 1997;4: 419–25.
15. Gleich LL, Gluckman JL, Armstrong S, et al. Alloantigen gene therapy for squamous cell carcinoma of the head and neck: results of a phase-1 trial. Arch Otolaryngol Head Neck Surg 1998;124:1097–104.
16. Gleich LL, Gluckman JL, Nemunaitis J, et al. Clinical experience with HLA-B7 plasmid DNA/lipid complex in advanced squamous cell carcinoma of the head and neck. Arch Otolaryngol Head Neck Surg 2001;127: 775–9.
17. Mapara MY, Sykes M. Tolerance and cancer: mechanisms of tumor evasion and strategies for breaking tolerance. J Clin Oncol 2004;22:1136–51.
18. Cooke KR, Kobzik L, Martin TR, et al. An experimental model of idiopathic pneumonia syndrome after bone marrow transplantation: I. The roles of minor H antigens and endotoxin. Blood 1996;88:3230–9.
19. Nakayama E, Uenaka A. Effect of *in vivo* administration of Lyt antibodies-Lyt phenotype of T cells in lymphoid tissues and blocking of tumor rejection. J Exp Med 1985;161:345–55.
20. Witherspoon RP, Storb R, Ochs HD, et al. Recovery of antibody production in human allogeneic marrow graft recipients: influence of time posttransplantation, the presence or absence of chronic graft-versus-host disease, and antithymocyte globulin treatment. Blood 1981;58:360–8.
21. Seddik M, Seemayer TA, Lapp WS. The graft-versus-host reaction and immune function. I. T helper cell immunodeficiency associated with graft-versus-host-induced thymic epithelial cell damage. Transplantation 1984;37:281–6.
22. Lum LG. The kinetics of immune reconstitution after human marrow transplantation. Blood 1987;69: 369–80.
23. Mapara MY, Kim YM, Wang SP, Bronson R, Sachs DH, Sykes M. Donor lymphocyte infusions mediate superior graft-versus-leukemia effects in mixed compared to fully allogeneic chimeras: a critical role for host antigen-presenting cells. Blood 2002;100: 1903–9.
24. Billiau AD, Fevery S, Rutgeerts O, Landuyt W, Waer M. Crucial role of timing of donor lymphocyte infusion in generating dissociated graft-versus-host and graft-versus-leukemia responses in mice receiving allogeneic bone marrow transplants. Blood 2002; 100:1894–902.
25. Michalek J, Collins RH, Durrani HP, et al. Definitive separation of graft-versus-leukemia- and graft-versus-host-specific $CD4^+$ T cells by virtue of their receptor β loci sequences. Proc Natl Acad Sci U S A 2003;100: 1180–4.
26. Zhang Y, Joe G, Zhu J, et al. Dendritic cell-activated $CD44^{hi}CD8^+$ T cells are defective in mediating acute graft-versus-host disease but retain graft-versus-leukemia activity. Blood 2004;103:3970–8.
27. Anderson LD, Jr., Savary CA, Mullen CA. Immunization of allogeneic bone marrow transplant recipients with tumor cell vaccines enhances graft-versus-tumor activity without exacerbating graft-versus-host disease. Blood 2000;95:2426–33.
28. Teshima T, Mach N, Hill GR, et al. Tumor cell vaccine elicits potent antitumor immunity after allogeneic T-cell-depleted bone marrow transplantation. Cancer Res 2001;61:162–71.
29. Luznik L, Slansky JE, Jalla S, et al. Successful therapy of metastatic cancer using tumor vaccines in mixed allogeneic bone marrow chimeras. Blood 2003;101: 1645–52.
30. Anderson LD, Jr., Mori S, Mann S, Savary CA, Mullen CA. Pretransplant tumor antigen-specific immunization of allogeneic bone marrow transplant donors enhances graft-versus-tumor activity without exacerbation of graft-versus-host disease. Cancer Res 2000;60:5797–802.
31. Teshima T, Hill GR, Pan L, et al. IL-11 separates graft-versus-leukemia effects from graft-versus-host disease after bone marrow transplantation. J Clin Invest 1999;104:317–25.
32. Edinger M, Hoffmann P, Ermann J, et al. $CD4^+CD25^+$ regulatory T cells preserve graft-versus-tumor activity while inhibiting graft-versus-host disease after bone marrow transplantation. Nat Med 2003;9: 1144–50.
33. Trenado A, Charlotte F, Fisson S, et al. Recipient-type specific $CD4^+CD25^+$ regulatory T cells favor immune reconstitution and control graft-versus-host disease while maintaining graft-versus-leukemia. J Clin Invest 2003;112:1688–96.
34. Matte CC, Liu J, Cormier J, et al. Donor APCs are required for maximal GVHD but not for GVL. Nat Med 2004;10:987–92.
35. Schmaltz C, Alpdogan O, Horndasch KJ, et al. Differential use of Fas ligand and perforin cytotoxic pathways by donor T cells in graft-versus-host disease and graft-versus-leukemia effect. Blood 2001;97:2886–95.
36. Zoller M. Immunotherapy of cancer for the elderly patient: does allogeneic bone marrow transplantation after nonmyeloablative conditioning provide a new option? Cancer Immunol Immunother 2004;53:659–76.
37. Stelljes M, Strothotte R, Pauels HG, et al. Graft-versus-host disease after allogeneic hematopoietic stem cell transplantation induces a $CD8^+$ T cell-mediated graft-versus-tumor effect that is independent of the recognition of alloantigenic tumor targets. Blood 2004;104:1210–6.
38. Faber LM, van Luxemburg-Heijs WS, Veenhof AF, Willemze R, Falkenburg JH. Generation of $CD4^+$ cytotoxic T-lymphocyte clones from a patient with severe graft-versus-host disease after allogeneic bone marrow transplantation: implications for graft-versus-leukemia reactivity. Blood 1995;86:2821–8.
39. Anderson BE, McNiff JM, Jain D, Blazar BR, Shlomchik WD, Shlomchik MJ. Distinct roles for donor- and host-derived antigen-presenting cells and costimulatory molecules in murine chronic graft-versus-host disease: requirements depend on target organ. Blood 2005;105:2227–34.
40. Rocha B, Grandien A, Freitas AA. Anergy and exhaustion are independent mechanisms of peripheral T cell tolerance. J Exp Med 1995;181:993–1003.
41. Huang AYC, Gulden PH, Woods AS, et al. The immunodominant major histocompatibility complex class I-restricted antigen of a murine colon tumor derives from an endogenous retroviral product. Proc Natl Acad Sci U S A 1996;93:9730–5.
42. Childs R, Clave E, Contentin N, et al. Engraftment kinetics after nomyeloablative allogeneic peripheral blood stem cell transplantation: full donor T-cell chimerism precedes alloimmune responses. Blood 1999; 94:3234–41.
43. McSweeney PA, Niederwieser D, Shizuru JA, et al. Hematopoietic cell transplantation in older patients with hematologic malignancies: replacing high-dose cytotoxic therapy with graft-versus-tumor effects. Blood 2001;97:3390–400.

BMC Genomics

BioMed Central

Methodology article

Open Access

"Per cell" normalization method for mRNA measurement by quantitative PCR and microarrays

Jun Kanno*†[1], Ken-ichi Aisaki†[1], Katsuhide Igarashi[1], Noriyuki Nakatsu[1], Atsushi Ono[1], Yukio Kodama[1] and Taku Nagao[2]

Address: [1]Division of Cellular and Molecular Toxicology, National Institute of Health Sciences, 1-18-1, Kamiyoga, Setagaya-ku, Tokyo 158-8501, Japan and [2]President, National Institute of Health Sciences, 1-18-1, Kamiyoga, Setagaya-ku, Tokyo 158-8501, Japan

Email: Jun Kanno* - kanno@nihs.go.jp; Ken-ichi Aisaki - aisaki@nihs.go.jp; Katsuhide Igarashi - igarashi@nihs.go.jp; Noriyuki Nakatsu - n-nakatsu@nihs.go.jp; Atsushi Ono - Atsushi@nibio.go.jp; Yukio Kodama - kodama@nihs.go.jp; Taku Nagao - nagao@nihs.go.jp

* Corresponding author †Equal contributors

Published: 29 March 2006

*BMC Genomics*2006, 7:64 doi:10.1186/1471-2164-7-64

Received: 06 November 2005

Accepted: 29 March 2006

This article is available from: http://www.biomedcentral.com/1471-2164/7/64

Abstract

Background: Transcriptome data from quantitative PCR (Q-PCR) and DNA microarrays are typically obtained from a fixed amount of RNA collected per sample. Therefore, variations in tissue cellularity and RNA yield across samples in an experimental series compromise accurate determination of the absolute level of each mRNA species per cell in any sample. Since mRNAs are copied from genomic DNA, the simplest way to express mRNA level would be as copy number per template DNA, or more practically, as copy number per cell.

Results: Here we report a method (designated the "Percellome" method) for normalizing the expression of mRNA values in biological samples. It provides a "per cell" readout in mRNA copy number and is applicable to both quantitative PCR (Q-PCR) and DNA microarray studies. The genomic DNA content of each sample homogenate was measured from a small aliquot to derive the number of cells in the sample. A cocktail of five external spike RNAs admixed in a dose-graded manner (dose-graded spike cocktail; GSC) was prepared and added to each homogenate in proportion to its DNA content. In this way, the spike mRNAs represented absolute copy numbers per cell in the sample. The signals from the five spike mRNAs were used as a dose-response standard curve for each sample, enabling us to convert all the signals measured to copy numbers per cell in an expression profile-independent manner. A series of samples was measured by Q-PCR and Affymetrix GeneChip microarrays using this Percellome method, and the results showed up to 90 % concordance.

Conclusion: Percellome data can be compared directly among samples and among different studies, and between different platforms, without further normalization. Therefore, "percellome" normalization can serve as a standard method for exchanging and comparing data across different platforms and among different laboratories.

Background

Normalization of gene expression data between different samples generated in the same laboratory using a single platform, and/or generated in different geographical

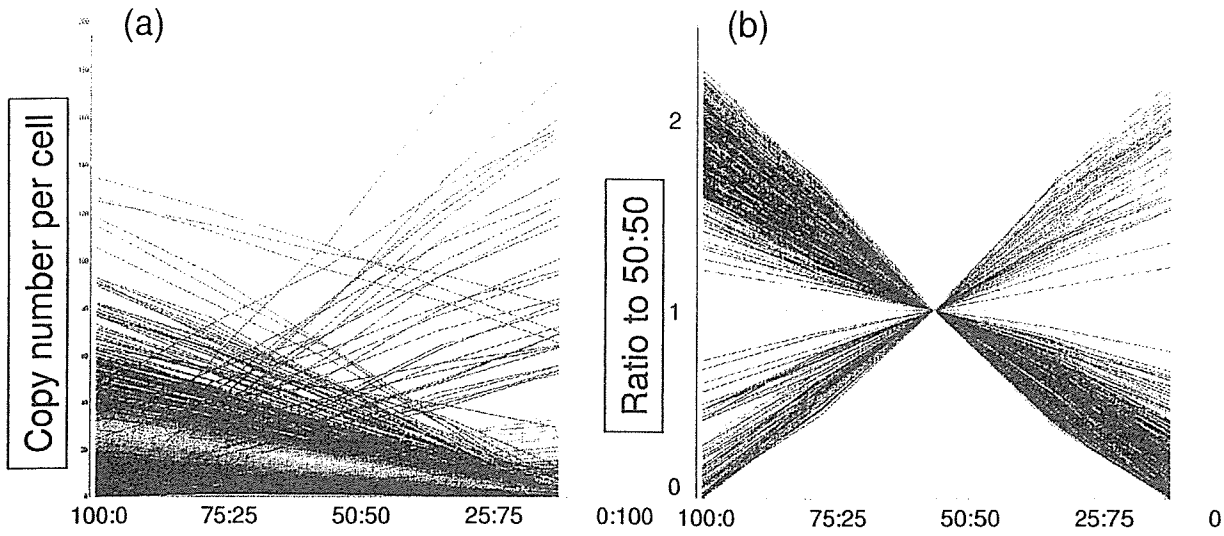

Figure 1
Dose-response linearity check by LBM. Dose-response linearity of the Affymetrix GeneChip by the LBM (liver-brain mix) sample set. Five samples, i.e. mixtures of mouse liver and brain at ratios of 100:0, 75:25, 50:50, 25:75 and 0:100, were spiked with GSC and measured by Affymetrix GeneChips Mouse430-2. Signals were normalized by the Percellome method as described in the text. Line graphs are in (a) copy numbers and (b) ratio to 50:50 sample for the top 1,000 probe sets with coefficient of correlation (R^2) closest to 1 among those having 1 copy or more per cell in the 50:50 sample (19,979 probe sets out of 45,101). The number of probe sets with $R^2 > 0.950$ was 8,655, and $R^2 > 0.900$ was 11,719.

regions using multiple platforms, is central to the establishment of a reliable reference database for toxicogenomics and pharmacogenomics. Transforming expression data into a "per cell" database is an effective way of normalizing expression data across samples and platforms. However, transcriptome data from the quantitative PCR (Q-PCR) and DNA microarray analyses currently deposited in the database are related to a fixed amount of RNA collected per sample. Variations in RNA yield across samples in an experimental series compromise accurate determination of the absolute level of each mRNA species per cell in any sample. Normalization against housekeeping genes for PCRs, and global normalization of ratiometric data for microarrays, is typically performed to account for this informational loss. Additional methods, such as the use of external mRNA spikes, reportedly improve the quality of data from microarray systems. For example, Holstege et al. [1] described a spike method against total RNA, based on their finding that the yields of total RNA from wild type and mutant cells were very similar. Hill et al. [2] reported a spike method against total RNA for normalizing hybridization data such that the sensitivities of individual arrays could be compared. Lee et al. [3] demonstrated that "housekeeping genes" cannot be used as a reference control, and van de Peppel et al. [4] described a normalization method of mRNA against total RNA using an external spike mixture. To achieve satisfactory performance they used multiple graded doses of external spikes, covering a wide range of expression, in order to align the ratiometric data by Lowess normalization [5]. Hekstra et al. [6] presented a method for calculating the final cRNA concentration in a hybridization solution. Sterrenburg et al. [7] and Dudley et al. [8] reported the use of common reference control samples for two-color microarray analyses of the human and yeast genomes, respectively. These are pools of antisense oligo sequences against all sense oligos present on the microarray. Instead of antisense oligos, Talaat et al. [9] used genomic DNA as a common reference control in studies of *E. coli*. Statistical approaches have been proposed for ratiometric data to improve inter-microarray variations, especially of non-linear relations [10]. However, because control samples may differ among studies, ratiometric data cannot easily be compared across multiple studies unless a common reference, such as a mixture of all antisense counterparts of spotted sense sequences is used [7-9]. Nevertheless, as long as the normalization is calibrated to total RNA, variations in total RNA profile cannot be effectively cancelled out. Although

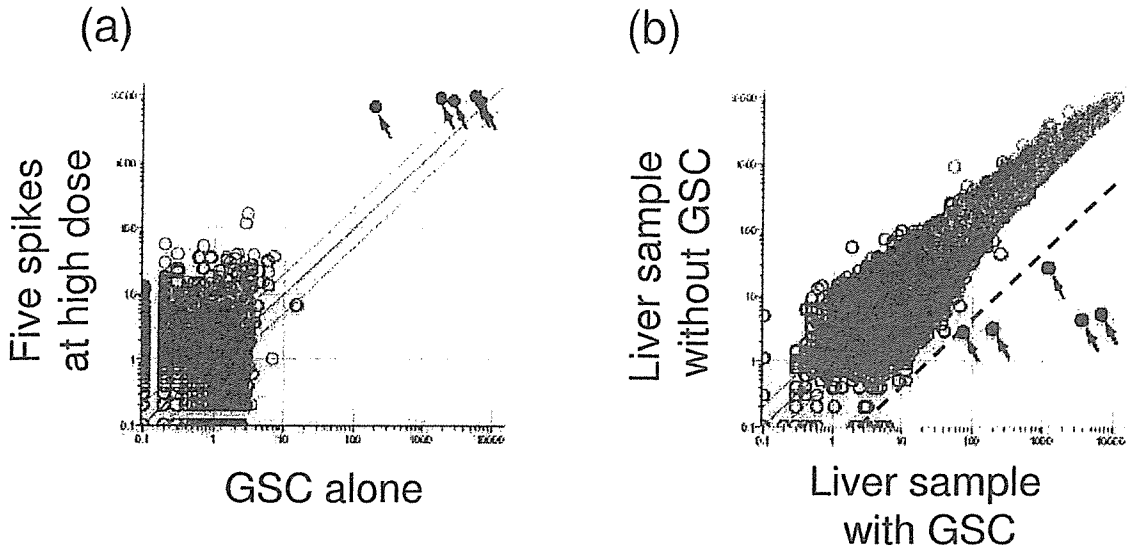

Figure 2
Cross-hybridization of GSC. Cross-hybridization of the GSC spike mRNAs to Affymetrix GeneChip. (a) A scatter plot of a blank sample with the GSC (horizontal axis) and a blank with the five spike RNAs at a high dosage (vertical axis) measured by MG-U74v2A GeneChips (raw values generated by Affymetrix MAS 5.0 software). The five spikes are indicated by black dots with arrows. Signals of the murine probe sets were below 20 on the horizontal axis, indicating negligible cross-hybridization of GSC spike mRNAs to the murine probe sets. (b) A scatter plot of a liver sample with GSC (horizontal axis) and without GSC (vertical axis) measured by MG-U74v2A GeneChips. The five spikes are again indicated by black dots with arrows. The dotted line is the 1/25 fold (4%) line. Cross-hybridization of mouse liver mRNAs to the GSC signals was considered negligible (less than 4%).

some of these reports share the idea that "absolute expression" and "transcripts per cell" should entail robust normalization, further practical development to enable universal application has been awaited.

Here, we report a method for normalizing expression data across samples and methods to the cell number of each sample, using the DNA content as indicator. This normalization method is independent of the gene expression profile of the sample, and may contribute to transcriptome studies as a common standard for data comparison and interchange.

Results

Dose-response linearity of the measurement system as a basis for the Percellome method

The fidelity of transcript detection is the key to this "per cell" based normalization method, which generates transcriptome data in "mRNA copy numbers per cell". The Q-PCR system was tested by serially diluting samples to confirm the linear relationship between Ct values and the log of sample mRNA concentration (data not shown). High density oligonucleotide microarrays from Affymetrix [11] were used in our experiments. We tested the linearity of the Affymetrix GeneChips using a set of five samples made of mixtures of liver and brain in ratios of 100:0, 75:25, 50:50, 25:75, and 0:100 (designated "LBM" for liver-brain mix). The results showed a linear relationship ($R^2 > 0.90$) between fluorescence intensity and input for a sufficient proportion of probe sets, i.e. about 37% of the probe sets in the older MG-U74v2 and 70% in the newest Mouse Genome 430 2.0 GeneChip were above the detection level (approximately one copy per cell) in the 50:50 sample (Figure 1) [see Additional files 1 and 2].

Dose-response linearity alone is not sufficient to generate true mRNA copy numbers. An important additional requirement is that the ratio of signal intensity to mRNA copy number should be equal among all GeneChip probe sets of mRNAs and PCR primers. The Q-PCR primer sets were designed to perform at similar amplification rates to minimize differences between amplicons. The melting

Table 1: The spike factors for various organs/tissues

Species	Organ/Tissue (adult, unless otherwise noted)	Spike Factor	total RNA/genomic DNA	SD
Mouse	Liver	0.2	211	46
Mouse	Lung	0.02	22	4
Mouse	Heart	0.05	-	-
Mouse	Thymus	0.01	8	2
Mouse	Colon Epitherium	0.05	105	30
Mouse	Kidney	0.1	-	-
Mouse	Brain	0.1	-	-
Mouse	Suprachiasmatic nucleus (SCN)	0.1	-	-
Mouse	Hypothalamus	0.1	63	4
Mouse	Pituitary	0.1	52	8
Mouse	Ovary	0.02	35	4
Mouse	Uterus	0.02	42	12
Mouse	Vagina	0.02	81	38
Mouse	Testis	0.15	56	7
Mouse	Epididymis	0.07	53	16
Mouse	Bone marrow	0.02	14	3
Mouse	Spleen	0.02	-	-
Mouse	Whole Embryo	0.15	97	36
Mouse	Fetal Telencephalon E10.5–16.5	0.1	48	9
Mouse	Neurosphere (E11.5–14.5)	0.03	42	10
Mouse	E9.5 embryo heart	0.15	58	15
Mouse	cell lines	0.2	-	-
Rat	Liver	0.2	-	-
Rat	Kidney	0.2	-	-
Rat	Uterus	0.04	56	5
Rat	Ovary	0.04	56	9
Human	Cancer Cell Lines	0.2	116	26
Xenopus	liver	0.03	-	-
Xenopus	embryo	0.15	-	-

temperature was set between 60° and 65°C with a product size of approximately 100 base pairs using an algorithm (nearest neighbor method, TAKARA BIO Inc., Japan), and the amplification co-efficiency (E) was set within the range 0.9 ± 0.1 (E = 2^{-(1/slope)}-1 on a plot of log2 (template) against Ct value). For the GeneChip system, the signal/copy performance of each probe set depended on the strategy of designing the probes to keep the hybridization constant/melting temperature within a narrow range, ensuring that the dose-response performances of the probe sets were similar (cf. http://www.affymetrix.com/technology/design/index.affx). Failing this, any differences should at least be kept constant within the same make/version of the GeneChip. Taking into consideration the biases that lead to imperfections in estimating absolute copy numbers in each gene/probe set, we developed normalization methods to set up a common scale for Q-PCR and Affymetrix GeneChip systems.

The grade-dosed spike cocktail (GSC) and the "spike factor" for the Percellome method

A set of external spike mRNAs was used to transfer the measurement of cell number in the sample (as reflected by its DNA content) to transcriptome analysis. For the spikes, we utilized five *Bacillus subtilis* mRNAs that were left open for users in the Affymetrix GeneChip series. The extent to which the *Bacillus* RNAs cross-hybridized with other probe sets was checked for the Affymetrix GeneChip system. The GSC was applied to Murine Genome U74Av2 Array (MG-U74v2) GeneChips with or without a liver sample. As shown in Figure 2, cross-hybridization between *Bacillus* RNAs and the murine gene probe sets was negligible [see Additional files 3 and 4]. Mouse Genome 430 2.0 Array (Mouse430-2), Mouse Expression Arrays 430A (MOE430A) and B (MOE430B), Rat Expression Array 230A (RAE230A), *Xenopus laevis* Genome Array and Human Genome U95Av2 (HG-U95Av2) and U133A (HG-U133A) Arrays sharing the same probe sets for these spike mRNAs showed no sign of cross-hybridization with the *Bacillus* probes (data not shown).

We prepared a cocktail containing in vitro transcribed Bacillus mRNAs in threefold concentration steps, i.e. 777.6 pM (for AFFX-ThrX-3_at), 259.4 pM (for AFFX-LysX-3_at), 86.4 pM (for AFFX-PheX-3_at), 28.8 pM (for AFFX-DapX-3_at) and 9.6 pM (for AFFX-TrpnX-3_at). By referring to the amount of DNA in a diploid cell and employing a "spike factor" determined by the ratio of

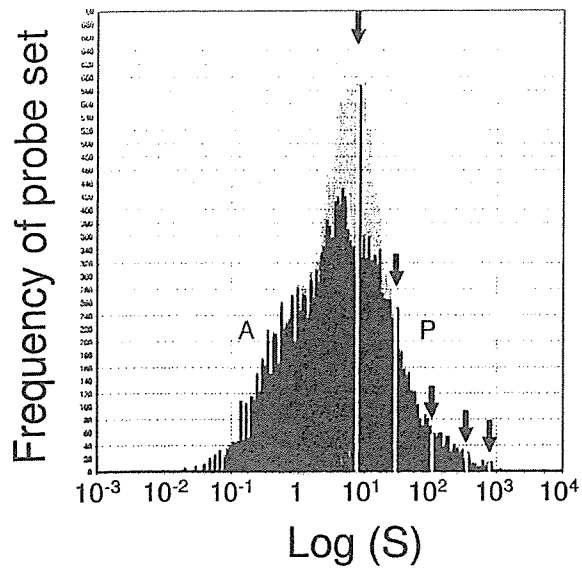

Figure 3
Positioning of GSC spike mRNAs in Affymetrix GeneChip dose-response range. A frequency histogram of the probe sets of Affymetrix GeneChip Mouse430-2 is shown. The histogram for all probe sets (gray) shows near-normal distribution. Blue columns are the "present" calls (P), red columns "absent" calls (A) and green "marginal" calls. The five yellow lines indicate the positions of the GSC spike mRNAs that are chosen to cover the "present" call range by a proper "spike factor".

total RNA to genomic DNA in a tissue type (Table 1), the spike mRNAs were calculated to correspond to 468.1, 156.0, 52.0, 17.3 and 5.8 copies per cell (diploid), respectively, for the mouse liver samples (spike factor = 0.2). The ratio of mRNAs in the cocktail is empirically chosen depending on the linear range of the measurement system and the available number of spikes. Here, we set the ratio to three to cover the "present" call probe sets of the Affymetrix GeneChip system (Figure 3).

We tested this grade-dosed spike cocktail (GSC) by Q-PCR and confirmed that the Ct values of the spike mRNAs were linearly related to the log concentrations (cf. Figure 4a), i.e. could be expressed as

$$Ct = \alpha \log C + \beta \quad \{1\}$$

The GSC was also tested by the GeneChip system and it was confirmed that the log of the spike mRNA signal intensities was linearly related to the log of their concentrations (cf. Figure 4b),

$$\log S = \gamma \log C + \delta \quad \{2\}$$

The linear relationship between the Ct values (Ct) and the log of RNA concentration (log C) was reasonable given the definition of Ct values (derived from the number of PCR cycles, i.e. doubling processes). The linear relationship between the log of GeneChip signal intensity (log S) and the log of RNA concentration (log C) was rationalized by the near-normal distribution of log S over all transcripts (cf. Figure 3).

Calculation of copy numbers of all genes/probe sets per cell

As described above, using a combination of DNA content and the spike factor of the sample, the GSC spike mRNAs become direct indicators of the copy numbers (C') per cell. When the samples were measured by Q-PCR or GeneChip analysis, the five GSC spike signals in each sample should obey function {1} for Q-PCR and function {2} for GeneChip with a good linearity. If the observed linearity was poor, a series of quality controls was performed and the measurement repeated. The coefficients of the functions were determined for each sample by the least squares method. Under the assumption that all genes/probe sets share the same signal/copy relationship, signal data for all genes/probe sets were fitted to the functions {1'} or {2'}, which are the individualized functions of {1} and {2} for each sample measurement (i).

$$Ct = \alpha i \log(C') + \beta i \quad \{1'\}$$

$$\text{Log } (S) = \gamma i \log(C') + \delta i \quad \{2'\}$$

(i = sample measurement no.)

The Q-PCR Ct values (Ct) and microarray signal values (S) of all mRNA species in the sample (i) are converted to copy numbers per cell (C') by the inverses of functions {1'} and {2'}, i.e. {3} and {4} below:

$$C' = B\text{^}((Ct-\beta i)/\alpha i) \quad \{3\}$$

for Q-PCR (Figure 4a).;

$$C' = B\text{^}((\log S-\gamma i)/\delta i) \quad \{4\}$$

for GeneChips (Figure 4b),

where B is the logarithmic base used in {1} and {2} (see Materials and Methods for details).

Real world performance of the Percellome method

The correspondence between Q-PCR and GeneChip was tested using a sample set from 2,3,7,8-tetrachlorodibenzodioxin (TCDD)-treated mice. Sixty male C57BL/6 mice